Aalto University
School of Chemical
Technology

School of Chemical Technology
Degree Programme of Materials Science and Engineering

Iiro Lehtiniemi

CORROSION AND WEAR OF MIXED METAL OXIDE ANODES IN ELECTROWINNING

Master's thesis for the degree of Master of Science in Technology submitted for inspection, Espoo, 20 November, 2013.

Supervisor **Docent , D. Sc. Jari Aromaa**

Instructor **M.Sc. (Tech) Istvan Galfi**

Aalto University
School of Chemical
Technology

Aalto University, P.O. BOX 11000, 00076 AALTO
www.aalto.fi

Abstract of master's thesis

Author	Iiro Lehtiniemi
Title of thesis	Corrosion and wear of mixed metal oxides in electrowinnig
Department	Material Science and Engineering
Professorship	Corrosion and hydrometallurgy
Code of professorship	MAK-85
Thesis supervisor	Docent, D.Sc. Jari Aromaa
Thesis advisor(s) / Thesis examiner(s)	M. Sc. (Tech) Istvan Galfi
Date	20.11.2013
Number of pages	89
Language	English

Abstract

The anode material in electrowinning of metals from sulfuric acid solution has traditionally been lead because of its high corrosion resistance. Most of the published research and development work of oxygen evolving anodes for electrowinning has focused on lead anodes since 1990´s. The mixed metal oxide anodes are more energy efficient than lead anodes. The operation of lead anodes is well known as they have been used for decades. The activity and operating time of the oxide anodes in sulfate based electrolytes is still an open question.

This work focuses on mixed metal oxide anode operation in sulfate-based electrowinning of base metals. The aim was to estimate the effect of dissolved metal ions on anode activity and lifetime. The applications and corrosion of anodes were reviewed and electrochemical characterization of IrO2-Ta2O5 anode was done in sulfuric acid solutions containing up to 60 g/L of copper, nickel, zinc or iron.

The effect of sulfuric acid concentration, different metal ions and different temperatures to polarization behavior of the anode were examined by polarization curves. The wear and corrosion of anode were experiment by long-term galvanostatic corrosion tests. The changes in anode activity were examined by cyclic voltammetry and electrochemical impedance spectroscopy.

The aim of this work was to find out if electrolyte conditions, especially metal ions, would change the active metal dissolution rate. One of the main factors affecting the dissolution rate is anode potential. The sulfuric acid concentration or metal ion concentration were not found to increase anode potential, but the addition of ferrous iron decreased anode potential.

Galvanostatic tests showed that anode activity decreased most clearly in sulfuric acid electrolytes containing copper or zinc. The same tendency was seen in nickel containing electrolytes but not as strongly. Anode activity decrease was detected as lower charge measured by cyclic voltammetry and higher charge transfer resistance measured by electrochemical impedance spectroscopy.

A major problem in anode testing is the selection of testing current density. The current densities used in electrowinning did not cause damages to the anodes. On the other hand, current densities that are tens of times higher do not lead to passivation in tens of hours. The solution could be use of extremely high current densities in the order of 10 kA/m2, but they may no longer describe the same wear and corrosion phenomena that happen in metal electrowinning.

Keywords DSA anodes, corrosion, wear, electrowinning, iridium oxide

Aalto-yliopisto
Kemian tekniikan korkeakoulu

Aalto-yliopisto, PL 11000, 00076 AALTO
www.aalto.fi

Diplomityön tiivistelmä

Tekijä Iiro Lehtiniemi		
Työn nimi Oksidianodien korroosio ja kuluminen talteenottoelektrolyysissä		
Laitos Materiaalitekniikan laitos		
Professuuri Korroosio ja hydrometallurgia		**Professuurikoodi** MAK-85
Työn valvoja Dosentti Jari Aromaa		
Työn ohjaaja(t)/Työn tarkastaja(t) DI Istvan Galfi		
Päivämäärä 20.11.2013	**Sivumäärä** 89	**Kieli** Englanti

Tiivistelmä

Talteenottoelektrolyysissä rikkihappopohjaisista liuoksista on perinteisesti käytetty lyijyä anodimateriaalina hyvän korroosion kestävyyden takia. Valtaosa talteenottoelektrolyysissä käytettävien happea kehittävien elektrodien tutkimuksesta ja kehityksestä on keskittynyt lyijyanodeihin 1990 luvulta lähtien. Lyijyanodien käyttäytyminen on hyvin tunnettua jo vuosikymmenten ajan. Oksidianodit ovat lyijyanodeja energiatehokkaampia. Oksidianodien aktiivisuus ja käyttöikä sulfaattipohjaisissa elektrolyyteissä on edelleen avoin kysymys.

Tämä työ keskittyy oksidianodien toimintaan perusmetallien sulfaattipohjaisessa talteenottoelektrolyysissä. Työn tarkoitus on arvioida liuenneiden metalli-ionien vaikutusta anodin aktiivisuuteen ja käyttöikään. Anodien käyttökohteita ja korroosiota on tutkittu kirjallisuuden kautta ja IrO2-Ta5 anodia tutkittiin kokeellisesti rikkihappoliuoksessa, aina 60 g/L pitoisuuteen kuparia, nikkeliä, sinkkiä tai rautaa.

Rikkihapon konsentraation, metalli-ionien ja lämpötilojen vaikutusta anodin polarisaatiokäyttäytymiseen tutkittiin polarisaatiokäyrillä. Anodin korroosiota ja kulumista tutkittiin pitkäaikaisilla galvanostaattisilla rasituskokeilla. Anodin aktiivisuuden muutoksia tutkittiin syklovoltammetrialla ja sähkökemiallisella impedanssi spektroskopialla.

Työn tarkoitus oli selvittää elektrolyytin ominaisuuksien, erityisesti metalli-ionien, vaikutusta aktiivisen metallin liukenemiseen. Anodin potentiaali on yksi tärkeimmistä vaikuttavista tekijöistä liukenemisen kannalta. Kokeissa ei havaittu että rikkihapon tai metallien konsentraatio kasvattaisi anodin potentiaalia. Rautaionien lisäyksen havaittiin laskevan anodin potentiaalia.

Galvanostaattiset rasituskokeet osoittivat että anodin aktiivisuus pieneni selvimmin rikkihappoelektrolyyteissä, jotka sisälsivät kuparia tai sinkkiä. Sama vaikutus oli havaittavissa nikkelipitoisessa elektrolyytissä, mutta ei yhtä voimakkaasti. Anodin aktiivisuuden pieneneminen havaittiin mitattuna matalampana varauksena syklovoltammetriakokeissa ja mitattuna korkeampana varauksena siirtovastuksessa sähkökemiallisissa impedanssi spektroskopiakokeissa.

Suurin haaste anodien tutkimisessa on kokeissa käytettävän virrantiheyden valitseminen. Talteenottoelektrolyysissä käytetyt virrantiheyden eivät aiheuta tuhoa anodille. Toisaalta kymmenkertaisesti korkeammat virrantiheydet eivät passivoineet anodia kymmenissä tunneissa. Ratkaisu voisi olla käyttää erittäin korkeita virrantiheyksiä, luokkaa 10 kA/m2, mutta silloin kokeet eivät välttämättä enää kuvaa samaa korroosiota ja kulumista mitä tapahtuu talteenottoelektrolyysissä.

Avainsanat Oksidianodi, korroosio, kuluminen, talteenottoelektrolyysi, iridiumoksidi

FOREWORD

This thesis was completed 1.2.2013 – 20.11.2013 in the Research Group of Corrosion and Hydrometallurgy in Aalto University. The thesis is part of the Wear and corrosion of DSA anodes in electrowinning project.

I would like to thank my supervisor D. Sc. (Tech) Jari Aromaa first of all for the possibility to work in the project and for sharing his extensive knowledge and interest in the subject. M. Sc. (Tech) Istvan Galfi I wish to thank for the numerous valuable advice he has given me during the thesis process. I would also like to thank Professor Olof Forsén for the possibility to work in the laboratory during my studies, which has significantly increased my knowledge and interest in the field of corrosion and hydrometallurgy.

Furthermore, I would like to thank the rest of the staff of the Research Group of Corrosion and Hydrometallurgy for the advice and technical support during this thesis.

At last, I would like to thank my family and friends for the support they have given to me during my studies and the making of this thesis.

Espoo, 20 November, 2013

Iiro Lehtiniemi

TABLE OF CONTENTS

1 INTRODUCTION

Electrowinning is one of the main methods to recover base metals from solutions. Electrowinning is commonly used in the production of copper, zinc, and nickel, but it is also applied in the production of cobalt and noble metals. In electrowinning metal is dissolved from the starting material using chemical or electrochemical leaching, the solution is purified from impurities that can disturb the deposition process, and metals are recovered using direct current. The deposition substrate can be same material as the deposited metal like starting sheets for copper or nickel. The substrate can also be a permanent material onto which the metal is deposited and then mechanically stripped of like stainless steel in copper production or aluminum in zinc production. The task of the anode is to maintain anodic reactions that in electrowinning of metals are typically oxygen evolution and chlorine evolution. The anode should be chemically and electrochemically stable and operate at low overpotential.

Electrodeposition of metals has been done industrially since 1840´s. First large scale raffination processes have been developed in 1860's for copper. The first electrowinning applications for metals production have been for zinc production since 1870-1880. Zinc electrowinning was developed during First World War and by 1970's leaching and electrowinning of zinc had become the major production method. Copper electrowinning started in the beginning of 1900's when Rio Tinto operated copper electrowinning using lead anodes and cathodes in dilute copper sulfate and sulfuric acid solution. Chuquicamata in Chile and Ajo in Arizona practiced copper electrowinning from leach solutions before First World War. Copper leach, solvent extraction and electrowinning process was taken into use in 1960's and it has become more and more important since 1980's. The INCO process for nickel matte anodes was developed in 1950's. In this process anode potential was so high that some oxygen was evolved leaching the anode. Currently nickel electrowinning is done mostly from chloride solutions and sulfate-based solutions are only few.

The anode material in electrowinning of metals from sulfuric acid solution has traditionally been lead because of their high corrosion resistance. During use the lead surface is oxidized resulting in electrochemically active PbO_2 layer. This layer prevents further oxidation and provides an electrochemically active and conductive material passing the anodic current. Most of the published research and development work of oxygen evolving anodes for electrowinning has focused on lead anodes since 1990´s. Electrowinning from chloride-based solutions is primarily used at certain plants to recover nickel, cobalt, and copper. In these electrolytes lead-based anodes are not as efficient as in sulfuric acid solutions. The anodes are usually different metal oxide anodes.

The mixed metal oxide anodes are more energy efficient than lead anodes. The operation of lead anodes is well known as they have been used for decades. The activity and operating time of the oxide anodes in sulfate based electrolytes is still an open question. This work focuses on mixed metal oxide anode operation in sulfate-based electrowinning of base metals. The aim was to estimate the effect of dissolved metal ions on anode activity and lifetime. The applications and corrosion of anodes were reviewed and electrochemical characterization of IrO_2-Ta_2O_5 anode was done in sulfuric acid solutions containing up to 60 g/L of copper, nickel, zinc or iron.

This work was financially supported by the Technology Industries of Finland Centennial Foundation Fund for the Association of Finnish Steel and Metal Producers.

2 COMPOSITE ANODES

Composite anodes mean metal substrate anodes coated with noble metals or metal oxides. The base metal is working as electric conductor and gives mechanic form and structural strength and electrochemically active coating is working as current feeder to the solution. Noble metal anodes are coated with platinum or platinum alloys and metal oxide anodes are mainly coated with mixtures of ruthenium oxide, iridium oxide, cobalt oxide, tin oxide, and various spinels and titanium oxide or tantalum oxide. Noble metal anodes have been used from 1950's and metal oxide anodes from the early 1970's. The benefits of the composite anodes compared to massive metal, graphite or magnetite anodes are wear resistance, better catalytic qualities and smaller size, which make them use easier in various applications. Higher cost can be taken as disadvantage of composite anodes.

Composite anodes are used in electrochemical process industry, surface finishing technology, environmental protection technology and cathodic protection in different environments. Reactions on the anode surface are mainly gas evolution reactions, in other words oxygen evolution or chlorine evolution depending on the solution. Anode manufacture technologies include thermolytic coating, diffusion coating, plasma spraying, electrolytic and autocatalytic coating and also sputtering. The most common manufacturing technology is thermolytic coating using metal salt solution. Technology was invented by Dutch Henry Beer in the late 1960's and he patented it with assist of Italian Oronzio de Nora Impianti Elettrochimici S.A. at England (Br.Pat 6490/67), Belgium (Belg.Pat. 710,551), Japan (Jp. Pat. 46-21884) and several patents in the United States during 1972-1973. De Nora company established subsidiaries for instance to the United States, Germany and Sweden. For that reason different anode manufactures products have been remarkably identical. Before 1990's manufactures were not able to develop own versions of anodes. Strict patent protection could have affected the development by making it not profitable.

There are many different abbreviations to oxide anodes. For example DSA (Dimensionally Stable Anode) was originally Diamond Shamrock Technologies S.A. company trademark

but commonly at these days DSA anodes means almost any oxide coated anode. At Japanese and Russian publications are used also their own abbreviations on oxide anodes. For example term OCTE (Oxide Coated Titanium Electrode) is used in Japanese literature to mixed oxide anodes and ROTO (Ruthenium Oxide-Titanium Oxide), RTOA (Ruthenium Oxide-Titanium oxide Anodes), TROA, ORTA and TRDA (Titanium-supported Ruthenium Dioxide Anode) are Russian terms to mixed oxide anodes.

A schematic structure of a mixed metal oxide anode is shown in Figure 1. The base material gives shape to the anode and provides current feed. The intermediate layer provides adhesion of active coating, current transfer tot active coating, and prevents oxidation of the base material surface. The purpose of the active coating is to maintain electrochemical reactions. Figure 2 shows examples of anode surfaces that can have compact (a) or cracked mud (b) morphology.

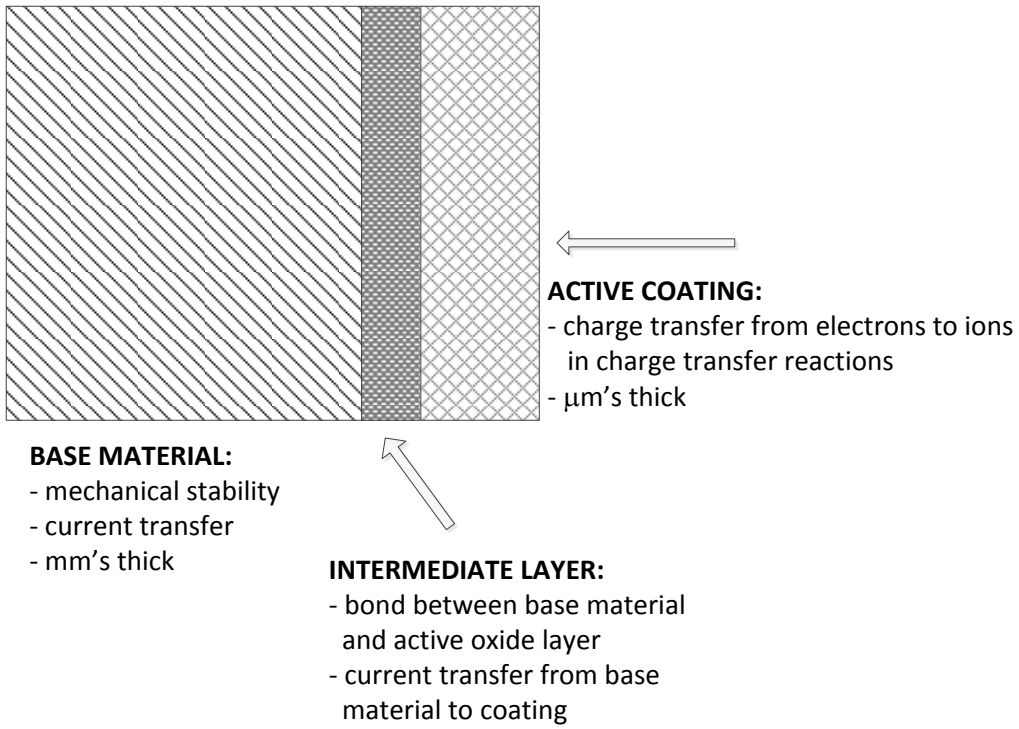

Figure 1. The schematic structure of a composite anode, after [Aromaa 1994].

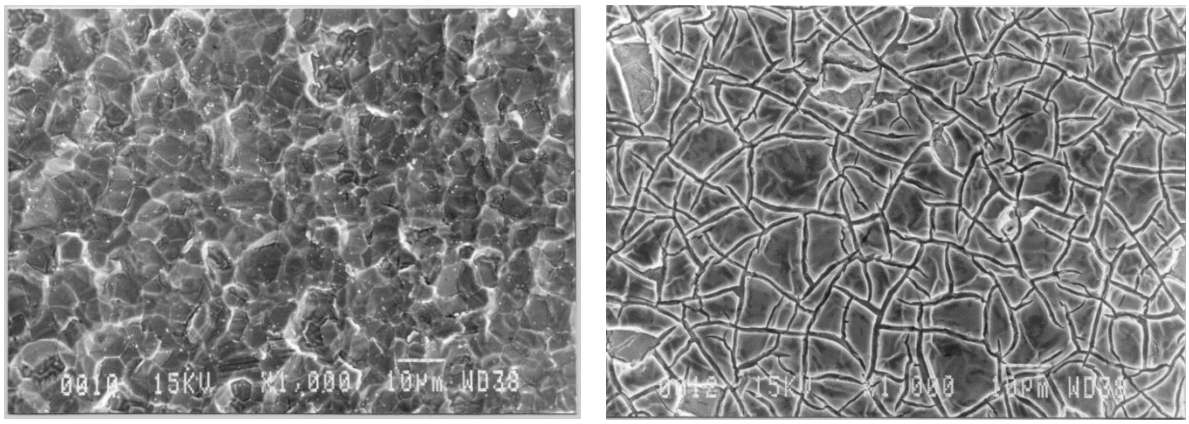

(a) (b)

Figure 2. Compact (a) and cracked-mud (b) structure of a RuO_2-TiO_2 oxide anode [Aromaa 1994].

2.1 Anode production and qualities

Despite various applications there are some general requirements that can be set to anode. Hine expresses following requirements to good anode materials [Hine 1985]:

- Low electrical resistance
- Good electrochemical activity
- Corrosion resistance
- Retain its form in application conditions.

Low electrical resistance reduces energy consumption of the process. Electrochemical activity decreases energy consumption and facilitates specific reactions improving selectivity of the process. Mechanical and chemical durability are essential requirements for trouble-free operation.

Anode properties are mainly determined by pretreatment of the base metal before it is coated by electrochemically active oxide layer, heat treatment temperature, amount of metal per deposition cycle, and thickness of the coating layer. These factors impact often more strongly anode's properties than chemical composition of the coating. Good electrochemically active layer structure is often cracked and porous to increase the surface area in contact to electrolyte. Electrochemical activity depends on the amount of active sites

in the coating that are in contact to electrolyte. Only the rutile-type oxides are considered electrochemically active, for example RuO_2, IrO_2, PtO_2, MnO_2, RhO_2 and PbO_2. From those oxides RuO_2, IrO_2 and RhO_2 are metallic conductors and PtO_2, MnO_2 and PbO_2 are semiconductors. Electrochemically active oxides that are used in anodes are commonly RuO_2 and IrO_2 [Matsumoto et. al. 1986] [Kotowski et. al. 1991]. During operation oxide layer forms on the surface of noble metal anode that acts as active oxide and protects the noble metal from dissolving. This phenomenon has been noticed for example with platinum whose surface will form a PtO_2 layer.

2.2 Anode materials

Mixed metal oxide anodes consist of mixture of active oxide and inert oxide that stabilizes the anode. In the development of anodes the focus has been in long time durability and selectivity. These qualities can't be actually modified by changing the active component because there is only limited number of alternative replacements to active compounds like ruthenium oxide and iridium oxide. For that reason the development of anodes has often focused on other components and their effect on the activity, stability and cost of the oxide anode. Different oxides are applied to different conditions case by case. To facilitate oxygen evolution in acidic solutions mixed oxides like RuO_2 + TiO_2 and RuO_2 + IrO_2 + TiO_2 have been used. TiO_2 has often been replaced by Ta_2O_5 to improve stability [Cardarelli 1998]. Oxide layers have usually only the pure oxide's basic crystal structure where composition, stoichiometry and qualities varying strongly [Trasatti 1987]. Ruthenium oxide is usually oxygen sub stoichiometric and iridium oxide oxygen trans-stoichiometric.

Almost all commercial oxide anodes are based on ruthenium oxide or iridium oxide. For oxide evolution in acidic solutions best long-lasting oxide anodes are based on iridium and tantalum oxides. IrO_2 based anodes are more stable for oxygen evolution but they have higher overpotential and are more costly than RuO_2 based anodes [Shrivastava 2008]. In neutral and alkaline solutions oxygen evolving anodes show life times that are long enough. Ruthenium or iridium never used as pure oxide. These oxides are the most expensive

components of the electrocatalytic coating. When used in aggressive solutions the active components lost by chemical or electrochemical corrosion could cause that the process is economically unprofitable. From at the beginning of development of oxide anodes noble metal oxides have been mixed with stabilizing oxides such as TiO_2, ZrO_2, Ta_2O_5 and SnO_2 that can be either conductors or insulators. Even though the addition of stabilizing oxide causes often reduction of electrochemical activity, the longer life time thus gained makes those coating more economical [Comninellis et. al. 1991].

2.3 Reactions of active oxides

Standard electrode potential between metallic ruthenium and Ru_2O_3 is 495 mV vs. SCE and between metallic ruthenium and RuO_2, reaction (1), it is 185 mV vs. SCE. Ergo, ruthenium oxide can reduce to metallic ruthenium if it's polarized enough to cathodic direction [Galizzioli et. al. 1974].

$$Ru + 2\ H_2O \leftrightarrow RuO_2 + 4\ H^+ + 4\ e^- \qquad (1)$$

The ruthenium dioxide RuO_2 can be produced only by oxidizing ruthenium metal at high temperature, heating ruthenium hydroxide at around 450 °C or oxidizing ruthenium chloride or sulfate at around 400 °C [Pourbaix 1966]. The rest potential of ruthenium dioxide in acidic solutions consists at reaction 2 [Galizzioli et. al. 1975].

$$2\ RuO_2 + 2\ H^+ + 2\ e^- \leftrightarrow Ru_2O_3 + H_2O \qquad (2)$$

Standard electrode potential of reaction (2) is 695 mV vs. SCE. In practice, the equilibrium reaction at electrode surface reaction is more likely (3)

$$RuO_2 + H^+ + e^- \leftrightarrow RuOOH \qquad (3)$$

The equilibrium between metallic iridium and iridium dioxide IrO_2 is described by reaction (4) [Pourbaix 1966],

$$Ir + 2\ H_2O \leftrightarrow IrO_2 + 4\ H^+ + 4\ e^- \quad (4)$$

The standard electrode potential of reaction (4) is 681 mV vs. SCE. If it is assumed that for IrO_2 and Ir_2O_3 equilibrium reactions are similar to those of ruthenium oxide reaction (2) the standard electrode potential would be 681 mV vs. SCE for reaction (5) [Pourbaix 1966].

$$2\ IrO_2 + 2\ H^+ + 2\ e^- \leftrightarrow Ir_2O_3 + H_2O \quad (5)$$

According to Pourbaix Ir_2O_3 oxidizes very fast to IrO_2 even in air so Ir_2O_3 occurrence is unlikely [Pourbaix 1966] and equilibrium of reaction (5) is strongly on the IrO_2 side. The iridium electrode shows also equilibrium between IrOOH and $IrO_2 \cdot x\ H2O$ (6) that is identical to ruthenium compound reaction (3). Reaction (6) is extremely reversible [Kelly et. al. 1990].

$$IrOOH + y\ H_2O \leftrightarrow IrO_2 \cdot x\ H_2O + H^+ + e^- + (y\text{-}x)\ H_2O \quad (6)$$

At high oxidizing potentials IrO_2 could oxidize further to iridate ion IrO_4^{2-} by reaction (7), which has standard electrode potential is 1812 mV vs. SCE.

$$IrO_2 + 2\ H_2O \leftrightarrow IrO_4^{2-} + 4\ H^+ + 2\ e^- \quad (7)$$

In acid chlorine-free solutions an anode that has been coated with ruthenium oxide doesn't last because of oxygen evolution. The reaction mechanism of oxygen evolution on RuO_4 which will react by releasing oxygen and ruthenium returns to RuO_2 form. RuO_4 is very soluble and it could also evaporate which could cause loss of ruthenium from the anode. According to Beck oxygen evolution on ruthenium oxide will happen by reaction mechanism (8)-(9) [Beck 1989b]:

$$RuO_2 + H_2O \rightarrow RuO_4 + 4\,H^+ + 4\,e^- \quad (8)$$

$$RuO_4 \rightarrow RuO_2 + O2 \quad (9)$$

Since all RuO_4 doesn't regenerate back, the oxygen evolution on ruthenium oxide anode causes inevitably a decrease in ruthenium oxide surface concentration. Kelly et. al. point out that with both ruthenium and iridium oxygen evolution mechanism is electrochemical oxide mechanism (see Chapter 4), where the second stage is rate controlling step [Kelly et. al. 1990]. In the electrochemical oxide mechanism active sites will oxidize to higher oxidization state compounds, which will release oxygen and the active site will regenerate.

2.4 Manufacturing parameters and their effects

A composite anode has two crucial interfaces: surface between electrocatalytic layer and base metal and surface between electrocatalytic layer and solution. The efficiency of electrocatalyst impacts both inner qualities of the system and the real active area of system. Anode manufacturing elements that result in anode activity are dissolved salts and solvent, concentration of solutions, spread technique of solution, number and thickness of coating layers, heat treatment time and temperature and heat treatment atmosphere. Factors that effect to the activity could have also impact to the durability of anode. For example active oxide layer can usually not be made over 25 µm thick because it would be mechanically too weak [Schrieber et. al. 1987].

Production and properties of the interface between base material and active layer also effect the life time of anode. This interface provides good adhesion between base material and active coating but at the same time the interface should be good current conductor from base material to coating and give good protection against corrosion on those areas of base material that are in contact to electrolyte. Especially processing of this surface before and after formation of the actual active oxide layer will make differences between various anodes manufacturer's products [Katowski et. al. 1991]. For example in patent FI 68090

[Beer et. al. 1979] are presented that this intermediate layer is thin noble metal oxide – titanium oxide layer, where concentration of the noble metal is clearly lower than in the actual active oxide layer. In patent FI 69123 [Hayfield 1980] is presented use of oxygen sub-stoichiometric tantalum oxide (Ta_2O_{5-x}) layer to prevent activation of titanium base material at cold seawater conditions.

2.4.1 The effect of active component

The Tafel slope values, apparent exchange current densities and potential ranges vary strongly depending on anode material, manufacturing methods and measurement conditions. Tafel slope value of thermolytically produced pure ruthenium oxide in 0.5 M sulfate solution was 40 mV and that of pure iridium oxide about 60 mV. The value of the slope started to increase clearly when there was more than about 60 mol-% of iridium dioxide [Angelinetta et. al. 1989]. The ruthenium oxide – iridium oxide anodes have been developed to be used for oxygen evolution in acid solutions. Idea of this noble metal oxide mixture is to combine the activity of ruthenium oxide and the stability of iridium oxide. It has been stated that with anodes that are produced thermolytically the Tafel slope of oxygen evolution will increase exponentially when the molar ratio of iridium oxide to ruthenium oxide increases.

Several authors have noted an inflection point in Tafel slopes. For example Yeo et al. measured Tafel slope values in 1.0 N H_2SO_4 for oxygen evolution and found two slope values depending on the potential, Figure 3. For RuO_2-based anode Tafel slope was 31–41 mV in the low potential region and 42–66 mV in the high potential region. The Tafel slope has lower value at lower potentials, and theoretically the Tafel slope for RuO_2 (110) plane has been calculated as 55 mV at low potential region and 105 mV at high potential region. The value of Tafel slope changes because rate-determining step of the oxygen evolution reaction changes. Based on theoretical calculations this change happens at 1.58 V [Fang 2010].

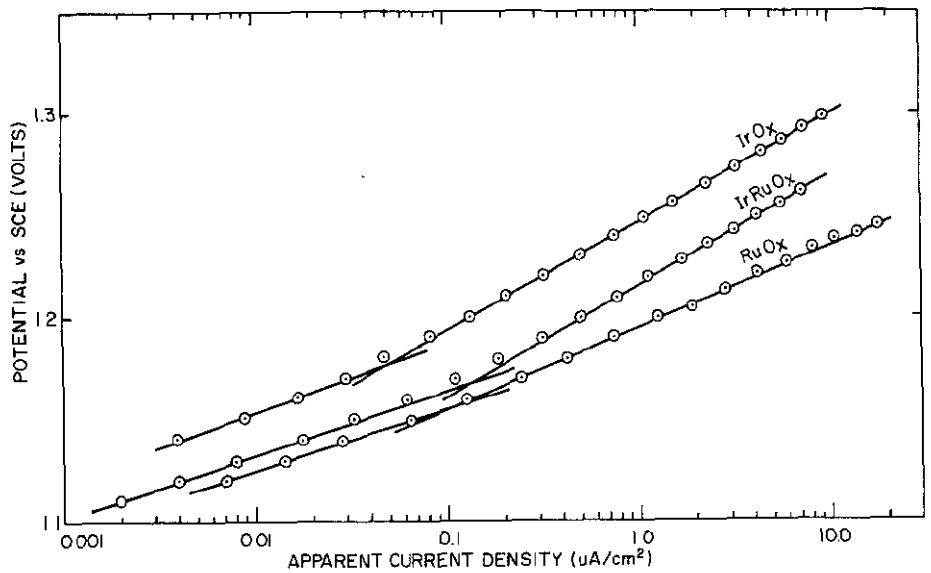

Fig. 1. Tafel plots for oxygen evolution on IrO_x, $IrRuO_x$, and RuO_x in 1.0*N* H_2SO_4 at 25°C.

Figure 3. Tafel plots for noble metal oxides IrO_x, RuO_x and $IrRuO_x$ [Yeo, 1981].

Shrivastava and Moats measured Tafel slopes in 0.5 M H_2SO_4 for RuO_2-TiO_2 anodes that contained 20 to 75 % RuO_2. The Tafel slope values at the high potential range, above 1.25 V vs. Ag/AgCl were 157-292 mV depending on anode composition and preparation method. Increasing the Ru content of the anode decreased Tafel slope value [Shrivastava 2009]. Current–potential curves for oxygen-evolution on $Ir_xTi_{1-x}O_2$ electrodes in 0.5 M H_2SO_4 were measured by Endo [Endo, 2002]. For x < 0:5 Tafel slope was not dependent on Ir concentration and that was 60 mV at E > 1.45 V. For x > 0:6 there were two Tafel slopes 90 mV at E < 1.45 V and 60–90 mV at E > 1.45 V.

For $Ru_xIr_{1-x}O_2$ coatings that were made by sputtering it was noticed that anode overpotential and Tafel slope increased when the concentration of iridium oxide increased. In 0.5 M sulfuric acid solution until the mole ratio of iridium was about 50 % the value b of Tafel slope was 60 mV/decade, which is the value of pure IrO_2. When the mole ratio of iridium decreased below 50 % of the slope decreased linearly to 40 mV/decade, which is the value of pure RuO_2 [Kötz et. al. 1986]. In galvanostatic experiments potential of anode

increased linearly when mole ratio of iridium increased. At the same galvanostatic experiments using 1 A/m^2 current density it was noticed that 20 mole percent ratio of iridium oxide could decrease the corrosion rate of RuO_2 to 4 percent of its initial value. In the experiments the corrosion rate of pure RuO_2 was about 180 nm/h and the corrosion rate of pure IrO_2 was about 3 nm/h [Kötz et. al. 1986].

2.4.2 The effect of inert oxide

The life time of anode has been increased by mixing inert oxides. For ruthenium oxide based anode either inert oxide or conducting oxide can be added. Usually the inert oxide has been TiO_2 but also SnO_2 has been used. There have also been studies of mixing tantalum oxides and zirconium oxides and some applications exist. The effect of type and amount of inert oxide to life time of anode has not been researched systematically [Comninellis et. al. 1991].

The additional inert oxide will effect crystal structure of active layer that forms at final heat treatment. TiO_2 and RuO_2 form metastable solid solution because both of them have similar rutile crystal structure. That is not $(Ru,Ti)O_2$ kind oxide mix but mixture of oxides. With long heat treatment times there can also form TiO_2, whose crystal structure is anatase. TiO_2 and IrO_2 form together solid solution but there is also pure iridium oxide in the active layer. With zirconium oxide ZrO_2 both RuO_2 and IrO_2 form oxide mix where oxides are not dissolved into each other. With tantalum oxide Ta_2O_5 both RuO_2 and IrO_2 form oxide mix with pure active oxide and amorphous phase [Comninellis et. al. 1991].

Type and amount of inert oxide have effect on electrical qualities, electrocatalytical qualities and life time of oxide layer. When relative part of titanium oxide increased in RuO_2+TiO_2 oxide mixture, the resistance of active layer increased exponentially but the main cause was probably the TiO_2 layer that formed on the surface of base material [Hine et. al. 1977]. It has been noticed that activity of thermolytically produced iridium oxide and ruthenium oxide anodes is affected by the inert oxide. The activity of TiO_2 containing

anode determined by cyclic voltammetry in 1 M sulfuric acid solution was highest when concentration of active oxide was around 10 mol-%. Activity of RuO_2 anode that was mixed either with ZrO_2 or Ta_2O_5 was highest when concentration of active oxide was 50 mol-%. Activity of IrO_2 anode that was mixed ZrO_2 was highest when concentration of active oxide was 40 mo-%t. Activity of IrO_2 anode that was mixed Ta_2O_5 was highest when concentration of active oxide was 70 mol-% [Comninellis et. al. 1991]. Inert oxides do affect the life time of anode, but because determining of life time with accelerated experiments is inaccurate and repeatability is poor, no accurate conclusions about the effect of inert oxide can be done. When studying thermolytically produced iridium oxide and ruthenium oxide based anodes in 30 percent sulfuric acid solution with galvanostatic experiments at 750 mA/cm^2, it was noticed that the stability of iridium oxide anodes increased in order $Ta_2O_5 > TiO_2 > ZrO_2$. Ruthenium oxide based anode stability increased in order $TiO_2 > ZrO_2 > Ta_2O_5$ [Comninellis et. al. 1991].

It has been stated that tin oxide SnO_2 stabilizes ruthenium oxide anodes and improves their selectivity to chlorine evolution [Hutchings et. al. 1984]. Based on the expected SnO_2 high oxygen evolution overpotential this should not happen. On the other hand, it has been noticed that when TiO_2 has been replaced by SnO_2 in RuO_2+TiO_2 anode with 30 mol-% ruthenium oxide, the activity to oxygen evolution has been improved [Onuchukwu et. al. 1991]. Because of contradictory experimental results it has been stated that effect of SnO_2 to the selectivity to chlorine evolution or oxygen evolution is so far unsolved.

2.4.3 The effect of heat treatment

Heat treatment temperature affects the electric conductivity of the active layer and the specific resistance of the active layer is at the lowest at about 400 °C. Polarization resistance of the active layer behaves similarly like specific resistance. Hine et. al. state that too low heat treatment temperatures will cause incomplete oxide conversion of ruthenium and too high temperatures will cause oxidization of the base material [Hine et. al. 1977]. Titanium should not be treated over 560 °C to prevent forming of insulating oxide layer

[Comninellis et. al. 1991]. Heat treatment time affects the electric conductivity of the anode in that way that at long times give enough time for oxygen to diffuse through the oxide to the surface of titanium where it could form insulating TiO_2 layer [Hine et. al. 1977].

Rising of the heat treatment temperature makes the oxidization of the base material surface easier, but on the other hand also the conditions of diffusion on the interface become better [Trasatti 1987]. So with appropriate preparation of the base material surface or premixing could modify electric and electrochemical qualities of the interface. On iridium oxide the rising the heat treatment temperature reduced exponentially the measured current density of oxygen evolution. At low temperatures treated anodes are more active but heat treatment at over 450 °C doesn't affect anymore to the activity. Basically temperature effect to the current density could be purely catalytic phenomenon, because thermolytically produced oxide layer has different qualities depending on temperature. On the other hand, great effect to the decrease of the activity can be caused by decrease of reactive area when surface layer be sintered and crystallized at higher temperatures [Trasatti 1987]. Heat treatment temperature could also effect to the crystal structure of the oxide layer and distribution of the atoms in the oxide layer. It has been noticed for $(Sn_{0,5},Ru_{0,25},Ir_{0,25})O_2$ electrodes that on the oxide layer surface the concentration of active ruthenium and iridium atoms decreases and concentration of inert tin atoms increases when heat treatment temperature is raised. Also the ratio of iridium increased more than ratio of ruthenium [Hutchings et. al. 1984].

3 LIFETIME OF ANODES

The life time of the electrochemically active coating is affected by base material's ability to form protective oxide layer that is also conducting and able to produce, corrosion resistant against for example fluorides, bromides, cyanates and nitrites, porosity or roughness effects of surface that affect effective current density and kinetics of wanted reactions that in turn determine the operating potential of the electrode surface and the stability of the coating [Comninellis 1991]. When developing oxide anodes for oxygen evolution in acid solutions it was noticed that platinum oxide and ruthenium oxide anode destruction were caused by oxidization and dissolution of the active component. Oxidization of platinum was less than oxidization of RuO_2. Compared to platinum and ruthenium, iridium is more stable and in practice iridium oxide anodes are destroyed when either base material dissolves or insulating layer forms between base material and active coating. When Pt or RuO_2 dissolves, the composition of active coating changes and mole ratio of inert oxide increases. This will cause increase of anode potential and increase of active component dissolution rate. Crucial to IrO_2 anode is ability of inert oxide to protect base metal from dissolving and for Pt and RuO_2 anodes the ability of inert oxide to stabilize the active component is important [Comninellis 1991].

The most common explanation to destruction of anode is loss of activity of the active layer, which causes increase of anode potential to area, where base material starts to dissolve. Activity of the active layer could drop because it becomes passive or the active layer has been dissolved or worn out. Loucka determined the life time of anode as the time, where anode potential doesn't increase significantly, that is less than 200-300 mV [Loucka 1977]. Typically, the life time of anode has been thought to be at its end when cell potential and energy consumption increase to so high values that using of the cell isn't any more economical. Hine et. al. state three different mechanism to destruction of anode: dissolution of coating, corrosion of base material causing breaking away of coating and oxidation of base material's surface isolating base material and active oxide layer from each other [Hine et. al. 1979]. According to Nidola the factors that affect the life time of anode are wear of

the active layer and declining of catalytical qualities of the active layer. Active layer wears for example by dissolving or by breaking away and catalytical qualities change for example when stoichiometry of coating changes or unwanted product layers precipitate on top of active layer [Nidola 1981].

Nidola divides causes of destruction of anode's active layer to direct causes and indirect causes [Nidola 1981]. Direct causes include breaking away of coating caused by penetration of oxygen, dissolution of coating caused by organic substances, oxidation of ruthenium to soluble or evaporable compounds, mechanical wear caused by solid substances, and short circuits, current reversals etc. Indirect causes include crevice corrosion of base material caused by either local decrease of pH in pores or increase in concentration of hazardous ions causing breaking away of coating, precipitation of excessive matter on top of coating causing passivation, poisoning or breaking away of coating caused by trapped gas bubbles, increase of anode potential when for example isolating oxygen bubbles penetrate to pores causing increase of anode potential to transpassive area, and formation of isolating interlayer on top of metal surface when oxygen atoms diffuse inward causing again increase of potential and breaking away of coating. Beck has in turn listed destruction mechanisms to oxide anodes as chemical dissolution of active oxide layer, destruction of Pb/PbO_2 type anodes caused by ion migration that goes through oxide layer, transpassive dissolution of active oxide layer, transpassive dissolution of passive layers, selective dissolution of passive intermediate layer, activation of base metal by localized corrosion, and formation of passivating intermediate layers [Beck 1989b].

A summary of anode destruction mechanisms is shown in Figure 4, but the possible destruction mechanisms of anodes can be simplified to two main causes: Decrease of surface concentration of the active component and increase of anode internal resistance. To estimate the life time of anode it is necessary to examine rate and effects of these phenomena. Many different studies have been done to define life time of anode and active

coating but no comprehensive explanation to destruction of anodes during acid oxygen evolution has been presented.

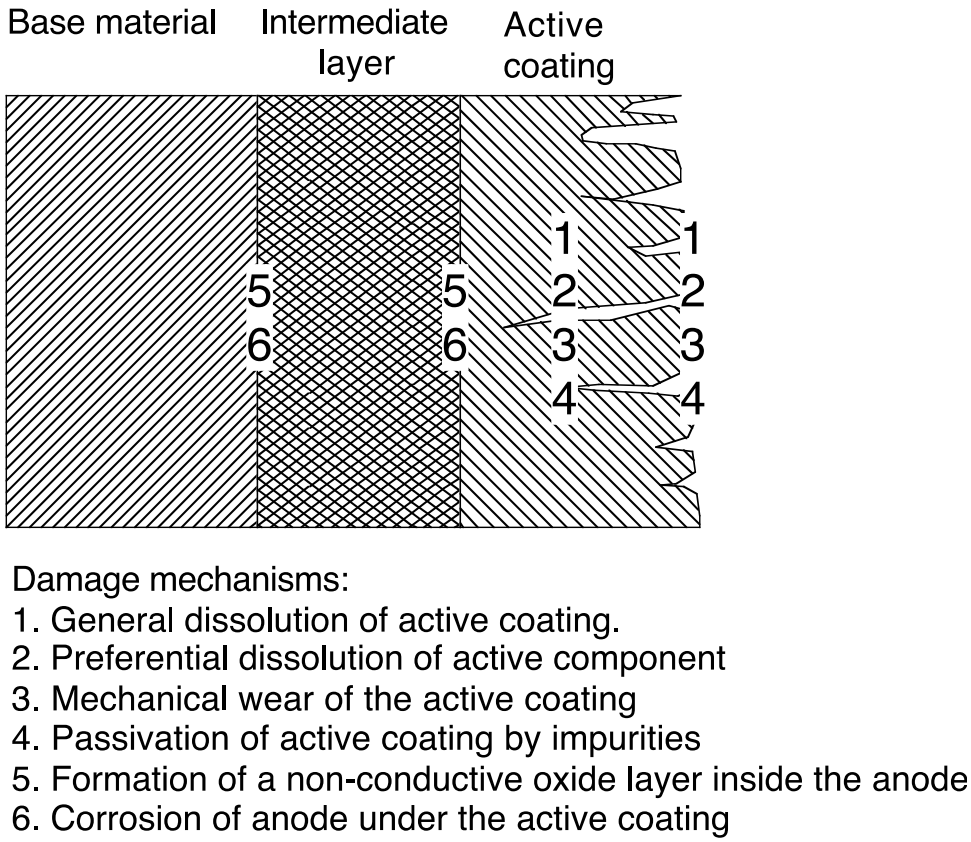

Figure 4. Anode damage mechanisms and affected areas, after [Aromaa 1994].

3.1 Operating factors affecting anode performance

he corrosion and wear of gas evolving DSA anodes are due to active coating consumption, mechanical damage due to intense gas evolution and internal passivation of base metal. According to [Krysa et al. 1996], [Alves et al. 1998] and [Lassali et al. 2000] at the first stage the rough outermost part of the oxide layer is destroyed by a combination of erosion and corrosion. Next, the more compact part of the active coating is used mostly by dissolution of the active component. During this process the interlayer containing less of the active metal gradually becomes thicker and less conductive. Finally, when the coating

layer is almost totally corroded, the poorly doped interface between base metal and active oxide passivates causing complete deactivation the of the anode. Hu et al. have shown that for a Ti/IrO_2–Ta_2O_5 anode in sulfuric acid both active oxide IrO_2 and stabilizing oxide Ta_2O_5 are lost in the beginning, thereafter IrO_2 is selectively lost and when anode passivates both oxides are lost, Figure 5. The cause of final passivation in these experiments was internal passivation due to TiO_2 formation [Hu 2002].

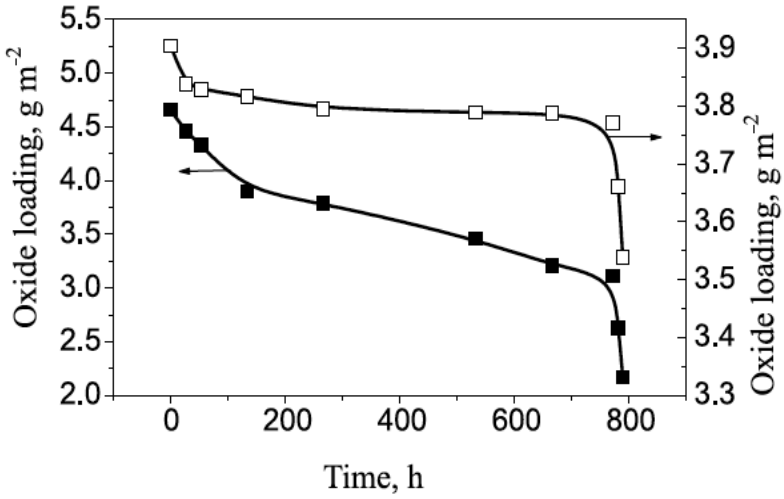

Fig. 4. Loading of IrO_2 (■) and Ta_2O_5 (□) in the oxide-coated Ti anodes during electrolysis.

Figure 5. Loss of active IrO_2 and stabilizing Ta_2O_5 during initial, stable and passivation phases [Hu 2002].

Anodes that become deactivated without total consumption of the active oxide layer are often porous and mainly deactivated by support metal passivation [Da Silva, 2004]. During long-term anodic polarization the Ti-noble metal contact can be progressively insulated by thickening of the TiO_2 barrier layer promoting passivation [Gueneay de Mussy, 2003].

The active oxide composition and oxide loading affect anode operating time. The higher is the relative amount of active component in the oxide the higher is the operating time. Often the operating time decreases sharply when the proportion of the active oxide is below a

critical value. For example for RuO_2-TiO_2 anodes this limit is around 20 mol-% [Klementeva, 1985]. The higher is the oxide loading [g/m^2] the higher is the operating time. The relation between active oxide loading and anode lifetime is usually not linear. For example during constant current testing the charge passed through the anode before passivation follows equation (10), where Q_A is the charge [C/cm^2] and c_A is oxide loading, and the exponent n is typically more than one [Beck 1989a].

$$Q_A = K \cdot c_A^n \tag{10}$$

The current density has direct effect on anode consumption. The higher is the current density, the faster is are the oxidation reactions on the active oxide and the faster will also be the rate of loss of the active oxide. The consumption rate has been found to follow logarithmic equation as shown in (11). Below a certain current density and thus also below a certain operating potential the active oxide dissolution rate is not significant. Above this application-dependent limit active component dissolution rate q [g/cm^{2}h] increases with current density [Gorodetskii et al. 1979]

$$q = m + p \cdot \log(i) \tag{11}$$

3.2 Dissolution mechanisms of active oxides

Bondar and Kalinovskii showed that on ruthenium oxide – titanium oxide anode the oxygen evolution reaction and ruthenium dissolution reaction run in parallel. Ruthenium was detected as gaseous ruthenium tetroxide [Bondar 1978]. Kötz et al. presented oxygen evolution and corrosion mechanism for ruthenium [Kötz 1983]. The oxygen evolution mechanism requires formation of RuO_4 compound that can escape as gas, Figure 6.

For iridium the starting point is $Ir(OH)_3$ and a deprotonation step $IrO(OH)_2$ is formed with Ir in the tetravalent state. Two additional deprotonation steps form IrO_3, with Ir in the hexavalent state. The oxygen is split off and simultaneous uptake of one water molecule leads back to tetravalent iridium. Alternatively to oxygen evolution, IrO_3 may dissolve into

the electrolyte as IrO_4^{2-} ion, Figure 7 (Kötz, 1984). Dimensionally stable anodes based on IrO_2 are stable above 1.85 V vs. RHE where RuO_2 has significant corrosion rate (Hine, 1979)(Kötz, 1983).

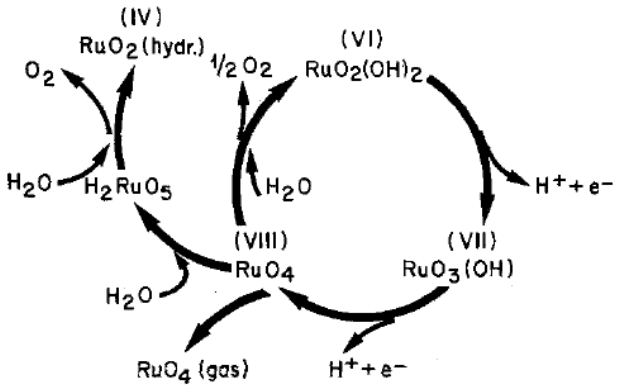

Fig. 7. Model for the oxygen evolution and corrosion on Ru and RuO_2 electrodes.

Figure 6. Redox reactions of ruthenium compounds. Formation of RuO_4 as intermediate compound leads to loss of Ru (Kötz, 1983).

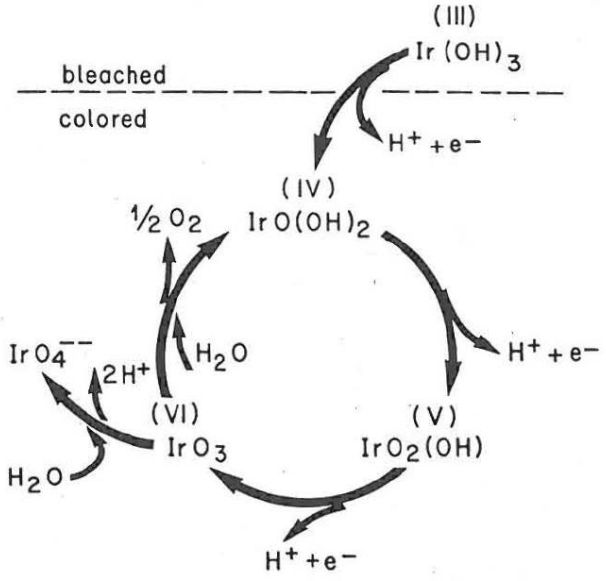

Fig. 6. Model for charge storage and oxygen evolution on iridium electrodes.

Figure 7. Redox reactions of iridium compounds, iridium is dissolved as IrO_4^{2-} (Kötz, 1984).

4 MECHANISMS OF OXYGEN EVOLUTION REACTIONS

Oxygen evolution reaction's mechanism is remarkably more complex than chlorine evolution reaction. The reason for that is that oxygen evolution reactions have several stages with intermediate products. The reaction paths for oxygen evolution on different anode materials are multistep reactions. Usually they require presence of more than one active site. The reaction path of oxygen evolution by decomposition of water in acid solutions involves electrochemical and chemical steps on active surface sites. Matsumoto and Sato list four reaction mechanisms of oxygen evolution in acid solutions and five in alkaline solutions [Matsumoto et. al. 1986]. In acid solutions the possible reaction mechanisms are following and S in them means the active site on the surface:

1. Electrochemical oxide mechanism

   $S + H_2O \rightarrow S\text{-}OH + H^+ + e^-$
   $S\text{-}OH \rightarrow S\text{-}O + H^+ + e^-$
   $2\ S\text{-}O \rightarrow 2\ S + O_2$

2. Oxide mechanism

   $S + H_2O \rightarrow S\text{-}OH + H^+ + e^-$
   $2\ S\text{-}OH \rightarrow S\text{-}O + S + H_2O$
   $2\ S\text{-}O \rightarrow 2\ S + O_2$

3. Krasilshchkov's mechanism

   $S + H_2O \rightarrow S\text{-}OH + H^+ + e^-$
   $S\text{-}OH \rightarrow S\text{-}O^- + H^+$
   $S\text{-}O^- \rightarrow S\text{-}O + e^-$
   $2\ S\text{-}O \rightarrow 2\ S + O_2$

4. Wade's and Hackerman's mechanism

   $2\ S + 2\ H_2O \rightarrow SO + SH_2O + 2\ H^+ + 2\ e^-$
   $SO + 2\ SOH^- \rightarrow 2\ S + SH_2O + O_2 + 2e^-$

The active site is usually a transition metal cation locating on the oxide surface. It works as a catalyst by either lower the activation energy of rate-controlling step or improves the

movement of electrons. The reaction path of oxygen evolution by decomposition of water in acid solutions involves electrochemical and chemical steps, reactions (12)-(14), and S denotes a surface active site, e.g. RuO_2 [Kelly 1987]. For ruthenium oxide the oxygen evolution follows electrochemical oxide mechanism. In the electrochemical oxide reaction mechanism (12)-(14) the rate determining step is (13), and step (13a) is typical for "compact" and (13b) for "cracked" morphologies (Lodi, 1978). [Lodi et al. 1978].

$$S + H_2O \rightarrow S - OH + H^+ + e^- \quad (12)$$

$$S - OH \rightarrow S - O + H^+ + e^- \quad (13a)$$

$$2\,S - OH \rightarrow S - O + S + H_2O \quad (13b)$$

$$2\,S - O \rightarrow O_2 + 2\,S \quad (14)$$

Oxygen evolution mechanism on RuO_2 at low voltages follows (15)-(17) [Panic 2006]

$$RuO_2 + H_2O \rightarrow RuO_2 - OH + H^+ + e^- \quad (15)$$

$$RuO_2 - OH \leftrightarrow RuO_3 + H^+ + e^- \quad (16)$$

$$2\,RuO_3 \leftrightarrow 2\,RuO_2 + O_2 \quad (17)$$

The reaction mechanism (15)-(17) is identical to the mechanism (12)-(14) with rate determining step (13b). For iridium oxide the most probable reaction mechanism is (18) to (20) with S denoting active surface site IrO_2 and S-O the higher oxide IrO_3 [Kulandaisamy et al. 1997].

$$S + H_2O \rightarrow S - O + 2H^+ + 2e^- \quad (18)$$

$$S - O \rightarrow O_{ads} + S \quad (19)$$

$$2\,O_{ads} \rightarrow O_2 \quad (20)$$

The reaction mechanism (18)-(20) is identical to the reaction mechanisms (12)-(13b)-(14) and (15)-(17).

The factors that have impact to oxygen evolution reaction electrocatalysis are for example the strength of the bonds between metal cations and oxygen in different adsorbed

intermediate products and transfer of electrons when different types intermediate products transform to others. It is believed that the structure of oxide layer affects the mechanism by which oxygen evolution happens. For example, if the ruthenium oxide surface has plenty of structural defects then oxygen evolution happens by oxide mechanism and if the oxide has only a small amount of structural defects then oxygen evolution happens by electrochemical oxide mechanism. In the electrochemical oxide mechanism the second electrochemical reaction stage determines reaction rate and in the oxide mechanism the first chemical reaction stage determines reaction rate. The final step where oxygen evolution happens is always fast [Lodi et. al. 1978].

Considering all the reaction mechanisms presented above, the final step releasing oxygen requires two active sites with a suitable intermediate product. Loss of the active sites will decrease the probability that two adjacent sites are found. This will mean slower rate of oxygen evolution. On the other hand, the anodes operate usually in constant current mode and when rate of oxygen evolution decreases, other reactions must start to consume the current that is delivered to the system. If oxygen evolution, or more correctly, the electrochemical steps involving production of intermediate products, is hindered then other oxidation reactions could be oxidation of base metal or transpassive oxidation of inert oxides. Both these reactions will cause anode damages, see Figure 4.

5 METHODS TO EVALUATE ANODE PERFORMANCE

The purpose of anode is to supply current to the electrochemical cell. Most of the hydrometallurgical processes use sulfuric acid solutions, and the main anodic reaction is oxygen evolution by decomposition of water. The term "electrocatalysis" refers to the beneficial influence of the electrode material on the reaction rate on the anode. On a practical basis any material resulting in a lower overpotential is regarded as a better electrocatalyst [Trasatti 1984], so the term is used mostly in a relative sense. Schultze defines electrocatalysis as acceleration of a charge transfer process by a catalyst which is present at a phase boundary, does not participate on the total reaction, and does not change the thermodynamics or mass transfer of the reaction [Schultze 1986]. The electrowinning cells operate usually in galvanostatic mode, i.e. the current density is kept constant and the anode potential is allowed to change freely. In addition to the thermodynamical potential, the anode potential includes activation and concentration overpotentials of all the electrochemical reactions and also resistance overpotentials due to hardware and internal ohmic resistance. A lower overpotential can thus result from a surface area related phenomenon, lower ohmic resistance or a true catalytic effect, which affects the reaction mechanism.

5.1 Anode activity

A permanent anode is an inhomogeneous electrode. The anode is a composite structure and when in contact with electrolyte, all different layers have their own responses to electrochemical excitation signals. A mixed metal oxide anode is based on titanium or other valve metal with an active coating. The active oxide coating itself is not homogeneous, because it is a mixture of several oxide phases. The morphology of the active coating is more or less porous, which means that kinetics of electrochemical reactions may vary on different parts of the anode surface.

A direct way to quantify anode activity is to measure the anode operational potential at constant current density. The electrolysis cell voltage ΔU consists of several components like thermodynamic (equilibrium) potential difference for the electrode reactions ΔE_{rev}, anodic and cathodic overpotentials, ohmic drop in the inter-electrode gap, in the electrodes and the connections ΔU_{Ω}, and the drift with time due to degradation of the electrode ΔU_t. For fresh electrodes the potential drift is zero. The cell voltage ΔU can be described by equation (21) (Trasatti, 2000). In equation (21) the overpotentials η_a and η_c and ohmic drop ΔU_{Ω} are directly dependent on current density.

$$\Delta U = \Delta E_{rev} + \eta_a + \eta_c + \Delta U_{\Omega} + \Delta U_t \qquad (21)$$

The lower is the anode potential at a given current density, the more active is the anode, Figure 8. Only the final potential is used to evaluate the anode performance. A potential decrease in the beginning is often due to penetration of electrolyte in the anode, which increases the reacting surface area. The potential approaches a steady value when both charge transfer rate and mass transfer rate reach constant values. The potential increase is due to these polarization effects. The result depends on experimental setup, as uncompensated ohmic resistance will be included in the measured potential. The method cannot separate the effects of intrinsic electrocatalysis, density of active sites and true surface area.

Steady-state current density in a potentiostatic experiment is another direct measure of anode activity. The schematic result of potentiostatic tests is shown in Figure 9. The current density decreases exponentially with time due to polarisation effects. The steady-state current density is a result of charge transfer and mass transfer polarization. Again, the effects of intrinsic electrocatalysis, true surface area and density of active sites cannot be separated. The uncompensated ohmic resistance can cause resistance overpotential, so that during the measurement the true anode potential is lower than the set potential.

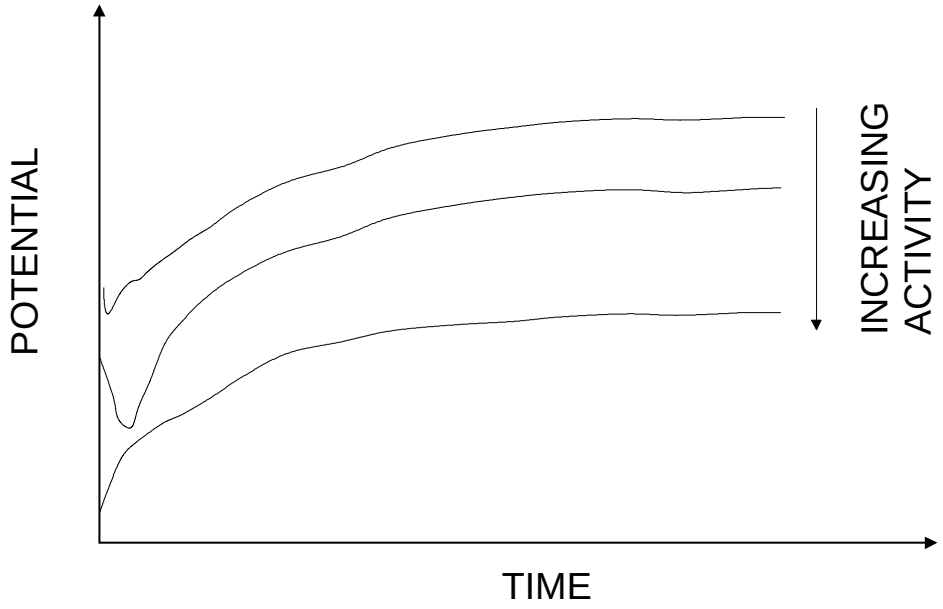

Figure 8. Schematic result of a galvanostatic test to evaluate anode activity. Lower potential means a better electrocatalyst [Aromaa 2002].

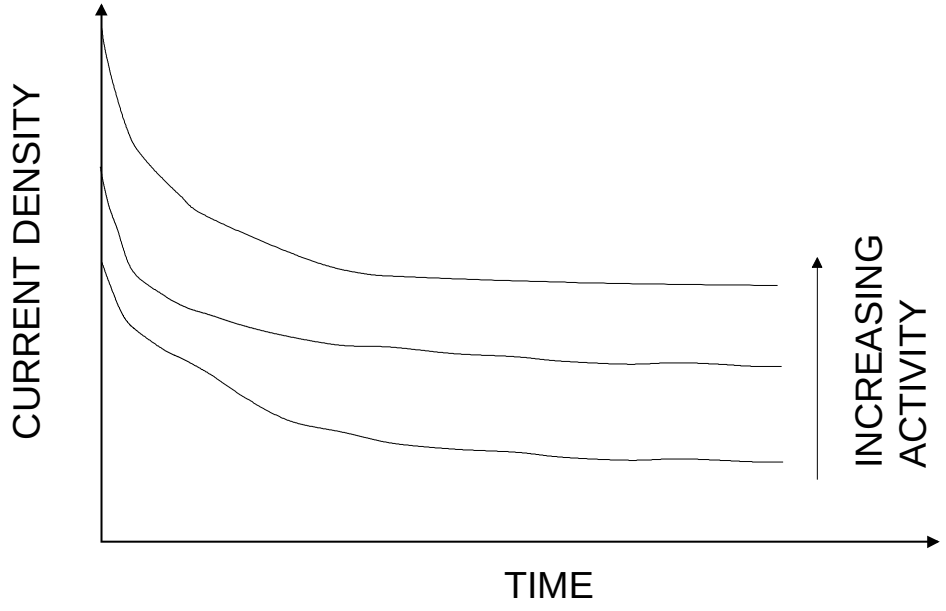

Figure 9. Schematic result of a potentiostatic test to evaluate anode activity. Higher current density means a better electrocatalyst [Aromaa 2002].

Tafel slope and exchange current density are two primary factors that describe the rate of charge transfer reaction. Exchange current density is a measure if the electrocatalytic properties, whereas Tafel slope is related to the reaction mechanism. A high exchange current density and a low Tafel slope value indicate a good electrocatalyst, Figure 10. The value of Tafel slope depends on the mechanism of the electrode reaction. Change of Tafel slope is a clear indication on changes in electrocatalytic effects.

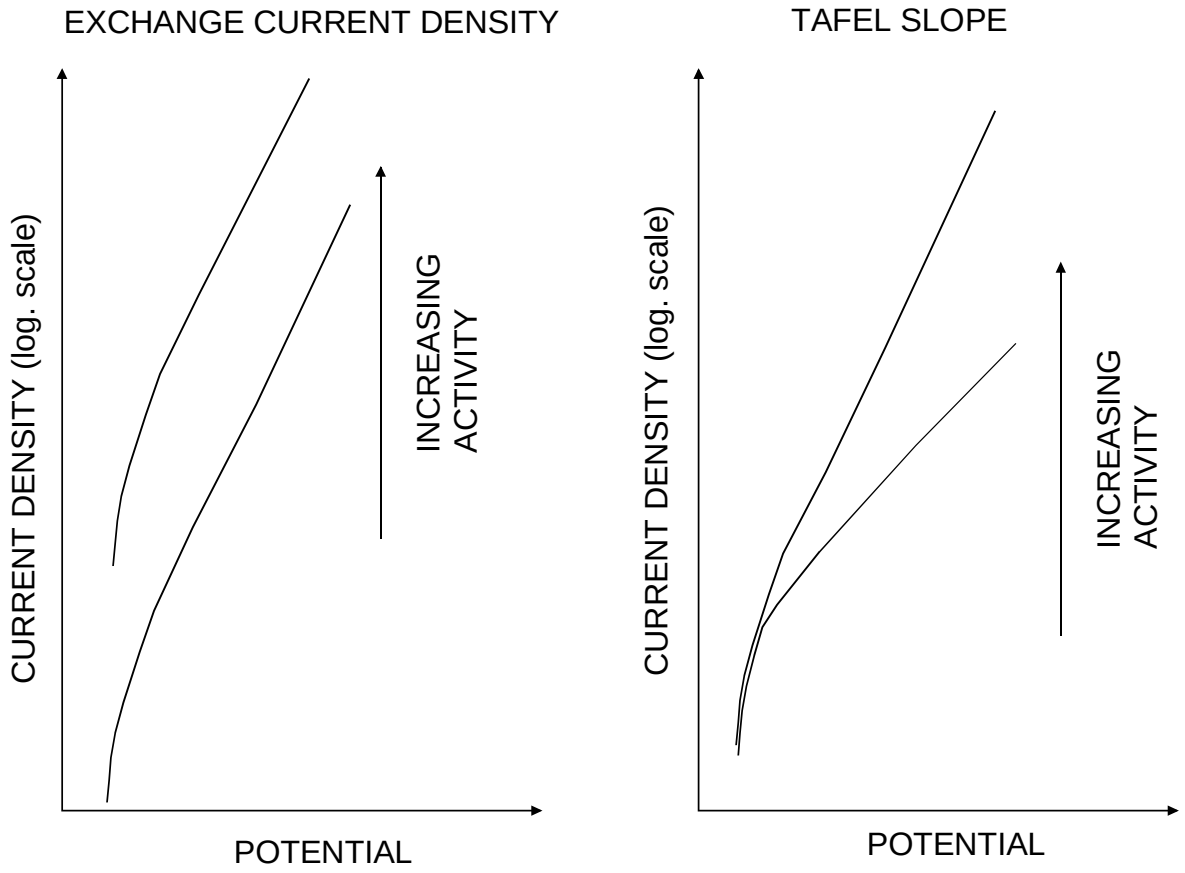

Figure 10. The effect of exchange current density and Tafel slope on anode activity. Higher current density at constant potential or lower potential at constant current density indicate a better electrocatalyst [Aromaa 2002].

Voltammetric charge recorded in a potential range where gas is not evolved can be used to estimate electrochemically active surface area [Trasatti 1984]. During a voltammetric measurement the surface is reversibly oxidized and reduced. For example, for ruthenium dioxide the voltammetric charge in acid solutions has been related to the proton exchange reaction (22) [Ardizzone 1990] and for iridium dioxide to equation (23) [Xu 2003]

$$RuO_x(OH)_y + \delta H^+ + \delta e \leftrightarrow RuO_{x-\delta}(OH)_{y+\delta} \quad (22)$$

$$2\ IrO_2 + 2\ H^+ + 2\ e^- \leftrightarrow Ir_2O_3 + H_2O \quad (23)$$

The charge spent during the potential sweep is assumed to be proportional to the surface area in contact with the electrolyte. If each active surface site undergoing oxidation and reduction during the potential sweep is also an active site for the gas evolution reactions, then the charge spent is a measure of the active surface area [Trasatti 1984]. The charge is dependent on the potential sweep rate. At lower sweep rates the charge is larger and it decreases towards a constant value when the sweep rate is increased. This might be related to the existence of less accessible regions, like pores and cracks, which are progressively not participating in reactions (22) or (23) as the sweep rate is increased [Ardizzone 1990]. The total charge is the sum of charges spent at "outer" (more accessible) and "inner" (less accessible) areas. By plotting the charge as inverse function of sweep rate using equation (24) it is possible to extrapolate the charge at infinite sweep rate. In equation (24) q_∞^* is the charge spent at easily accessible surface sites. By plotting the charge according to equation (25) it is possible to extrapolate the charge at zero sweep rate. In equation (25) q_0^* is equal to the total charge spent in the surface sites and in the pores [Ardizzone 1990].

$$q^*(v) = q_\infty^* + A \bullet \left(\frac{1}{\sqrt{v}}\right) \quad (24)$$

$$\frac{1}{q^*(v)} = \frac{1}{q_0^*} + B \bullet \sqrt{v} \quad (25)$$

Figure 11 shows examples of cyclic voltammograms and Figure 12 examples of the charges determined for IrO_2-Ta_2O_5 anode at different compositions. The results of Figure 12 show that the anode has maximum activity, that is highest charge, at around 60% IrO_2 [Xu 2003].

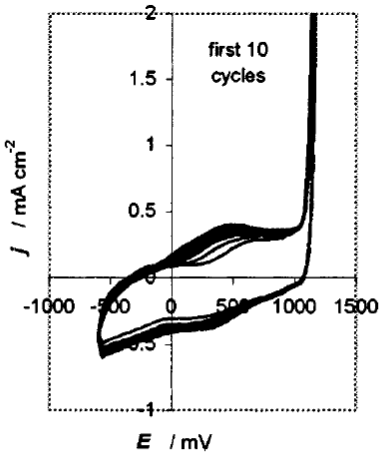

Figure 4. Cyclic voltammetric curves of IrO_2-Ta_2O_5 (Ir:Ta = 70:30) electrode with continuous cycling.

Figure 11. Cyclic voltammograms for IrO_2-Ta_2O_5 anode for determination of relative anode area [Xu 2003].

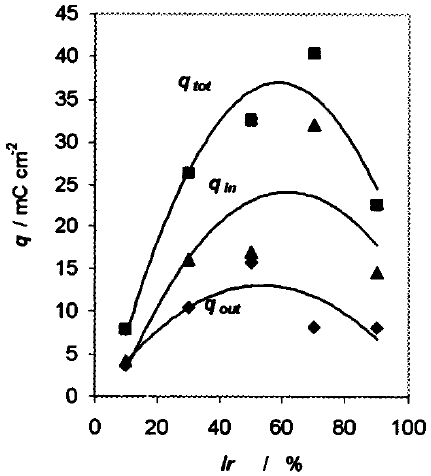

Figure 7. Total, outer, and inner surface charges as a function of Ir content in the IrO_2-Ta_2O_5 electrodes.

Figure 12. Inner, outer and total charges for a IrO_2-Ta_2O_5 anode with varying IrO_2 content [Xu 2003].

Electrochemical impedance spectroscopy allows separation of different electrochemical factors of the system under study. Thus it is theoretically possible to estimate anode activity by measuring charge transfer resistance, to estimate anode surface area by measuring capacitance and to estimate possible internal passivation from the shape of the impedance spectrum. For example, the loss of outer porous part of the oxide active layer could be seen in the decrease of capacitance (surface area related) and increase in charge transfer resistance (reaction rate related). Analysis of the impedance spectrum is based on equivalent circuit that has resistances, capacitances and inductances related to different physical and electrochemical factors of the surface. For example Da Silva et al. used equivalent circuit in Figure 13. R_Ω is the uncompensated solution resistance, the time constant (R_f-CPE1) describes the intermediate layer between base material and active oxide, the time constant (R_{ct}-CPE2) describes charge transfer reaction, and L is inductance seen in the high frequency domain [Da Silva 2004]. (R_f-CPE1) is seen in the high frequency domain and (R_{ct}-CPE2) in the low frequency domain.

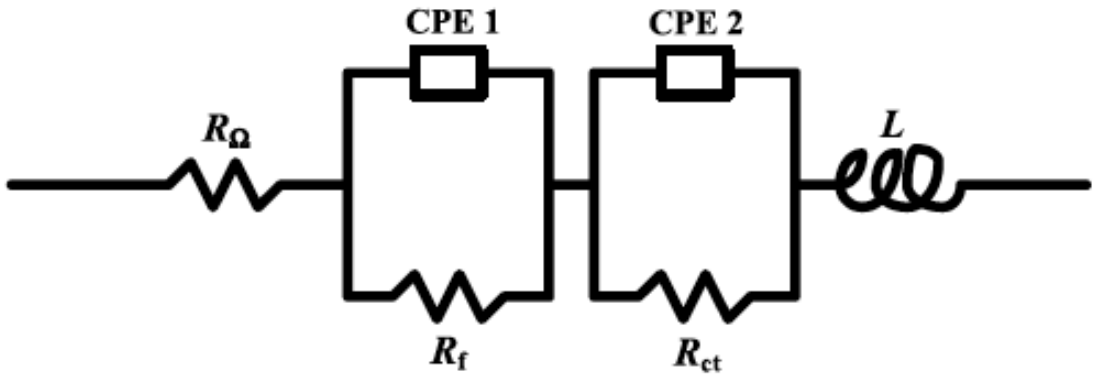

Fig. 10. Equivalent circuit used to describe the electrode response.

Figure 13. Equivalent circuit used in analysis of electrochemical impedance spectroscopy of DSA anodes [Da Silva 2004].

The components of an equivalent circuit are related to density of active sites and roughness factor. The charge transfer resistance R_{ct} and double layer capacitance C_{dl} described by CPE 2 in Figure 13 are dependent on applied potential and time. The charge transfer

resistance $R_{ct} = K/q^*$, where K is a function of exchange current density taken as average interfacial resistivity for the charge transfer process ρ_{ct} (Ω·mol/cm), average electron transfer distance d ($(0.3–2.0)\cdot10^{-11}$ cm) and surface concentration of the active sites $[S]_S$ (mol/cm^2). Considering also the effect of polarization, the charge transfer resistance at a certain potential becomes (26) [Da Silva 2004]

$$R_{ct} = \left\{\frac{\rho_{ect} \cdot d}{[S]_S}\right\} \cdot \exp\left(\frac{-\alpha F \eta}{RT}\right) \quad (26)$$

According to equation (26) the charge transfer resistance of the anodic reaction decreases or the anode activity decreases when interfacial resistivity of the charge transfer process at equilibrium potential ρ_{ect} decreases, the average electron transfer distance d decreases, surface concentration of the active sites $[S]_S$ decreases or anodic overpotential η increases. The double layer capacitance C_{dl} is related to the average interfacial permittivity ε (F/cm), surface area A and thickness of the double layer d_{dl}. The interfacial permittivity and double layer thickness are assumed constant and double layer capacitance can be estimated using equation (27).

$$C_{dl} = \varepsilon \cdot A_G \cdot rf/d_{dl} \quad (27)$$

The surface area in equation (27) is taken as geometric surface area A_G multiplied by roughness factor rf [Da Silva 2004]. During operation the anode surface area can change. This will result in changes in area of active coating in contact with the electrolyte. If no of the active coating is lost this change can be considered as change in roughness factor. If part of the coating detaches the surface area changes can be much larger and the capacitance changes can also be due to changes in permittivity.

Figure 14 shows an example of measured impedance spectrum as Nyquist plot. The Nyquist plot shows typical two semicircles associated with the two time constants shown in the equivalent circuit in Figure 13. The smaller high frequency domain semicircle is describes the interface film resistance and the larger low frequency domain semicircle the charge transfer resistance on the active oxide [Da Silva 2004].

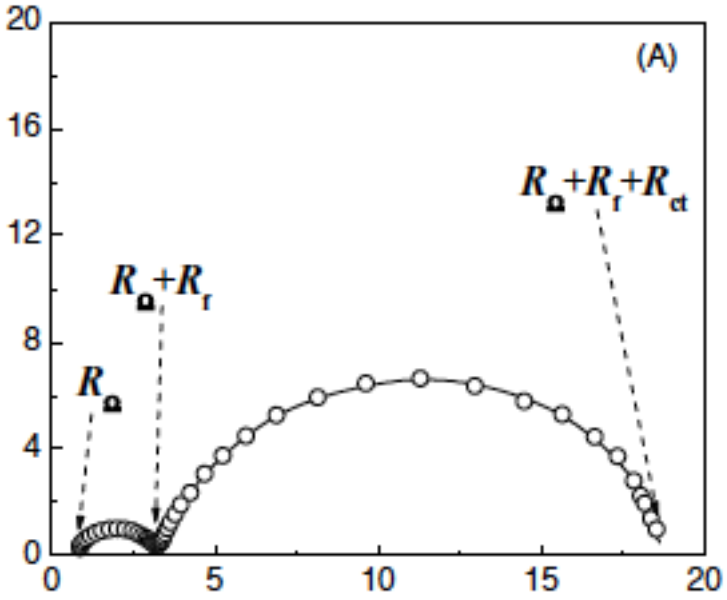

Figure 14. Nyquist plot for a composite anode in the frequency domain 10 mHz – 100 kHz showing high frequency semicircle for internal interface and low frequency semicircle for charge transfer on active oxide [Da Silva 2004].

Figure 15 shows typical impedance spectra for RuO_2-TiO_2 anodes with different compositions [Aromaa 1994]. On these RuO_2 anodes only one time constant, resulting from the oxygen evolution reaction, was seen when polarized. The impedance increased with decreasing RuO_2 concentration, and for the titanium sheet the impedance was about one order of magnitude higher than for 5 mol-% RuO_2 anode that had the lowest amount of active oxide. The capacitive region shifts to higher frequencies as the RuO_2 concentration decreases. The capacitive region shifts clearly to higher frequencies, when RuO_2 concentration is below 10 mol-%. In these cases the impedance spectrum is no longer describing only oxygen evolution as the inert TiO_2 phase begins to affect. The capacitance of the inert TiO_2 phase is several orders of magnitude higher than the capacitance of the active RuO_2 phase. This change can indicate also progressive loss of the active oxide as more of the TiO2 becomes in contact with the electrolyte. The loss of active oxide could be seen as increase of impedance.

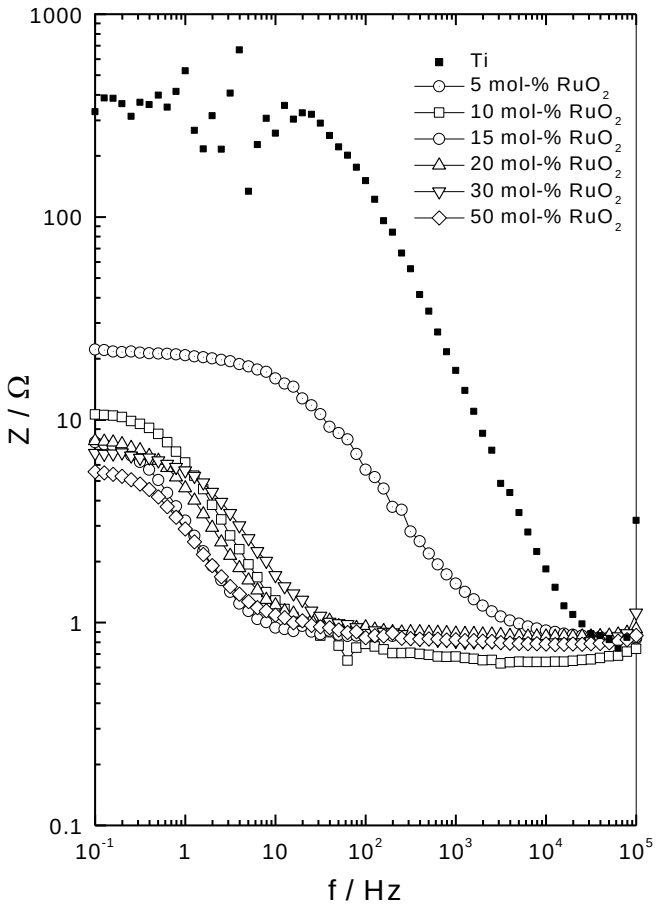

Figure 15. Galvanostatic impedance spectra at i = 2 mA/cm^2 for RuO_2-TiO_2 anodes with different compositions. 1-M H_2SO_4, T = 25 ºC, N_2-purged [Aromaa 1994].

5.2 Anode operating time

The composite anode operating time as taken as the time, after which the operating voltage or cell voltage becomes too high. The anode wear and corrosion are generally accepted to follow three steps:

1. Initial loss of poorly detached particles from the surface
2. Steady state loss of active compounds from the surface
3. Final passivation due to oxide formation inside the anode. This stage can also lead to detachment of active oxide layer.

The lifetime of a composite anode is usually taken as years. For example Moats estimated that in copper electrowinning the composite anode lifetime must be 1-3 years to be competitive [Moats 2008]. The service life of an insoluble anode is often determined under conditions of accelerated corrosion, using a high constant current and measuring the potential against time response, *cf* [Hine 1979], [Alves 1998], [Lassali 2000]. The current densities vary depending on anode type and environment and they can be as high as several kA/m^2. Highest current densities have been in the order of 100 A/cm^2 that corresponds to 1000 kA/m^2 and the anodes failed within minutes [Beck 1989a]. Extremely high current densities have been deemed not to be suitable for accelerated testing. The testing current density is a compromise between conditions of anode application and testing time. Testing of electrowinning anodes at current densities of kA/m^2 means use of 10 higher current densities than what are used in metals production.

Hine et al. showed that the time to failure is a double logarithmic function of current density, $\log(TTF) = a - b \cdot \log(i)$ [Hine 1979]. Beck noticed same dependency to a certain current density, above which the service life is constant [Beck 1989a]. Chen & Chen proposed that service life of a RuO_2-SnO_2-Sb_2O_5 anode for oxygen evolution in acid solution is inversely related to current density so that service life $\propto 1/i^n$, where n ranges from 1.4 to 2.0 [Chen 2005]. The anode lifetime correlates with the charge that passes through. The lifetime is shorter, when operating at higher current density even the charge is the same [Beck 1989a]. Kokoulina et al. suggested that corrosion rate of ruthenium oxide based anode increases at the high potential range with higher Tafel slope [Kokoulina 1978]. Krysa et al. showed that iridium dissolution rate and IrO_2-Ta_2O_5 anode lifetime had linear dependence [Krysa 1996]. These results show that anode testing at high current densities accelerates anode destruction but the test conditions may produce different damage mechanisms that are seen in practical applications.

Examples of anode testing at constant current are shown in Figures 16 to 19. Figure 16 shows tests of IrO_2-Ta_2O_5-SnO_2 anodes in chlorate solution. The composition of the inert oxide has an effect on anode operating time but the operating time is not a linear function of anode composition [Lassali 2000].

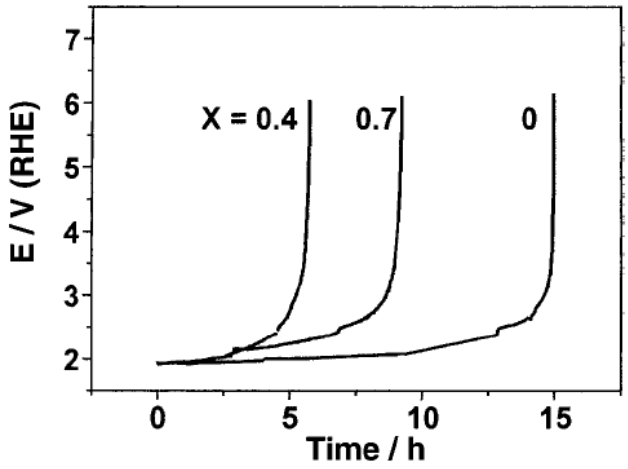

Fig. 1. Representative potential – time curves as function of the nominal composition of $Ir_{0.3}Ti_{(0.7-x)}Sn_xO_2$ electrodes in 1.0 mol dm^{-3} $HClO_4$. $j = 0.8$ A cm^{-2}.

Figure 16. The effect of anode composition on anode operation time [Lassali 2000].

Figure 17 shows and example with test by stepwise increase of current density. The current densities were 1 to 100 A/dm^2. Ruthenium based anodes were initially more active but they lost activity faster than platinum based anodes [Beck 1989a].

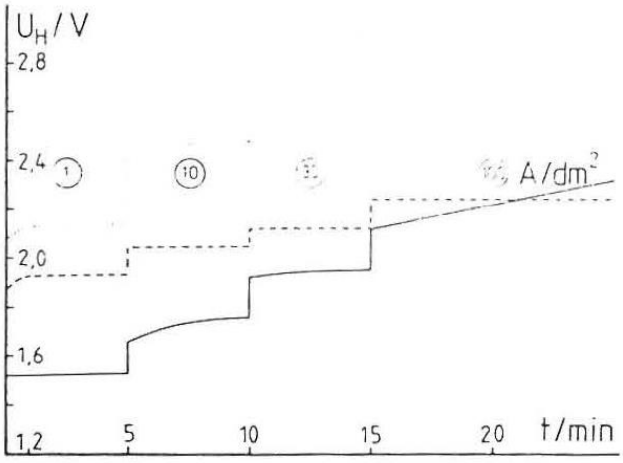

FIG. 4. Galvanostatic polarization of activated titanium anodes in 10 wt% H_2SO_4 at 25°C.
——— Ti/RuO_2, 5 g m^{-2}; ------ Ti/PtO_x, 5 g m^{-2}; ..... Ti·PtO_x, 0.5 g m^{-2}.

Figure 17. Stepwise current increase test for Ru and Pt-based anodes [Beck 1989a].

Figure 18 shows an example of testing of IrO_2 anode on aluminium substrate. The end of life of the anode is taken as the point, where anode potential reaches 10 V [Bock 2000].

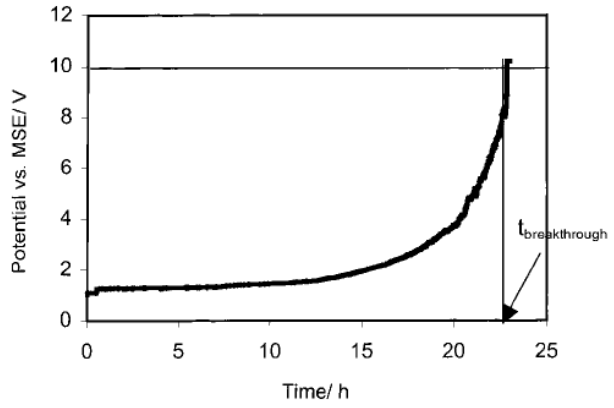

Fig. 1. Typical potential–time transients for a Al/IrO_2 (550 °C) anode at 100 mA cm^{-2} in 0.5 M H_2SO_4.

Figure 18. Testing of an Al/IrO_2 anode, where anode lifetime is taken as point, where anode potential reaches 10 V [Bock 2000].

Figure 19 shows an example of IrO_2 based anodes with different inert oxides. The testing current density is very high but still the test times are hundreds of hours [Chen 2001].

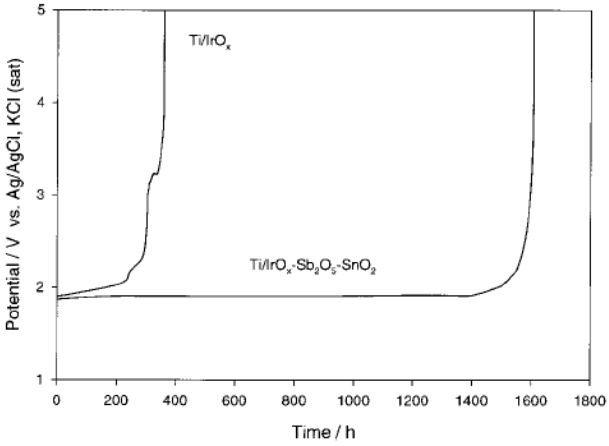

Figure 1. Accelerated life test comparison between Ti/IrO_x–Sb_2O_5–SnO_2 and Ti/IrO_x in 3 M H_2SO_4 solution under 1 A cm^{-2} at 35 °C.

Figure 19. Examples of testing of IrO_2 anodes with different inert oxides [Chen 2001].

The examples shown in Figures 16-19 point out several factors that must be considered when selecting test conditions for accelerated anode lifetime test. The test current density should be reasonably high considering the application. Too high current density can change the damage mechanisms and then the tests may not be relevant. On the other hand, the anode lifetimes are high and therefore also test times corresponding to actual applications are high. The Figure 19 indicates that in concentrated acid close to industrial electrowinning electrolytes and current densities almost 100 times more than those of electrowinning the test times can be well over 1000 hours which means several weeks. It is also common to use stepwise increases of current density starting from levels that are close to those of the application. Some of these test arrangements have been done using identical increases of current density, whereas others use increases by a factor of ten. The endpoint is usually taken as the sharp increase of anode potential. Sometimes this is tied to a certain potential value and sometimes not.

6 EXPERIMENTAL

6.1 Test materials

The anode material was iridium coated titanium wire with 3 mm diameter. In Figure 20 is presented a SEM image of the anode surface. It can be see that surface structure of anode is "cracked mud" structure, which is typical to oxide coated anodes. The surface structure forms during the final oxidation process of the anode manufacture. The cracked structure improves activity of the anode by increasing the active surface area.

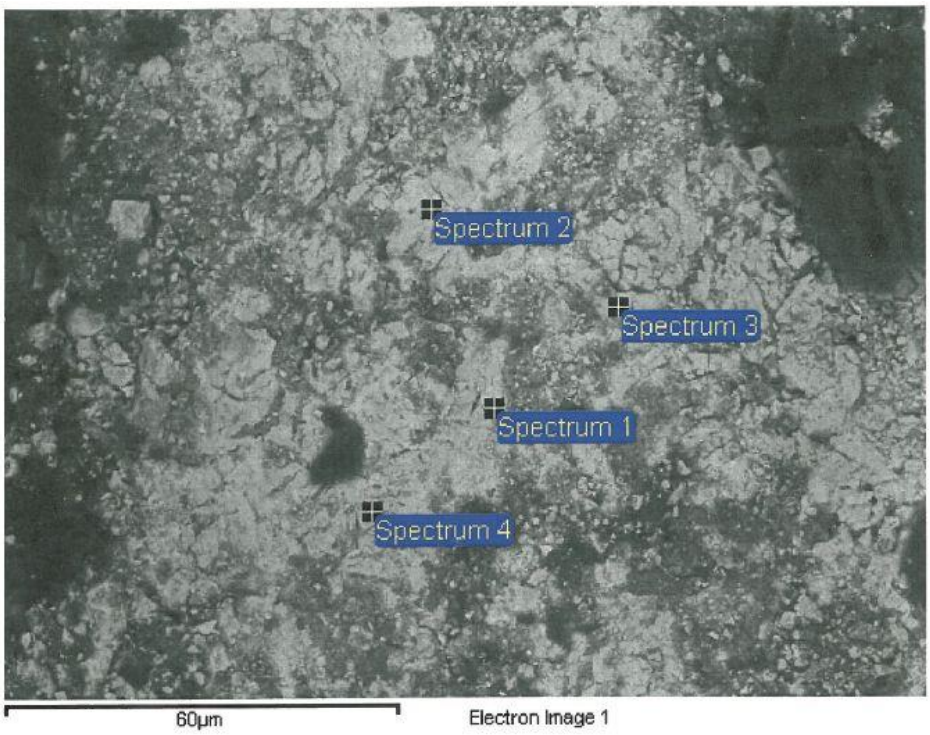

Figure 20. Surface of the test material and analysis points.

Analysis results of the anode surface are presented in Figure 20 and Table 1. The anode was analyzed to contain approximately 13 weight percent iridium, 15 weight percent

tantalum and 3 weight percent titanium. Iridium is the active component, tantalum is the inert component and titanium is structural component. The anode material compounds are typically IrO_2, Ta_2O_5 and TiO_2. The amount of active noble metals is typical for the DSA anodes.

Table 1. SEM analysis of the anode sample.

Spectrum	O	Na	Cl	Ca	Ti	Zr	Ta	Ir
Spectrum 1	64.68	0.66	1.91	0.24	3.66	0.31	14.03	14.51
Spectrum 2	62.80	0.36	1.29	0.22	9.00	0.39	16.31	9.62
Spectrum 3	67.16	1.43	2.36	0.42	1.42		14.02	13.20
Spectrum 4	62.61	0.86	2.03	0.31	3.19		15.72	15.27
Max.	67.16	1.43	2.36	0.42	9.00	0.39	16.31	15.27
Min.	62.61	0.36	1.29	0.22	1.42	0.31	14.02	9.62

The samples were prepared from the wire by cutting 37 mm and 21 mm long pieces. One end was threaded and connected to a copper wire. The other end was insulated with a small piece of Teflon to limit the active surface area to known value. The end of the 23 mm and 7 mm long cylinder electrodes were thus isolated from solution and sample was easily changed. Sample area in most of tests was 2.16 cm^2 and in few last tests 0.69 cm^2 because higher current densities were needed. The sample holder and anode sample are shown in Figure 21.

The electrolytes were made using p.a. and reagent grade chemicals and distilled water. Sulfuric acid solutions were made from p.a. 95-98% sulfuric acid (Sigma-Aldrich UN 1830). For metal sulfate solutions reagent grade chemicals were $FeSO_4 \cdot 7H_2O$ (Merck EMSURE 103965), $ZnSO_4 \cdot 7H_2O$ (Sigma-Aldrich Z4750) and $CuSO_4 \cdot 5H_2O$ (Sigma-Aldrich 209198). For nickel sulfate solutions were used technical grade $NiSO_4 \cdot 6H_2O$ from Norilsk Nickel. Before the polarization curve and the activity measurements solutions were purged with 99.99% pure nitrogen.

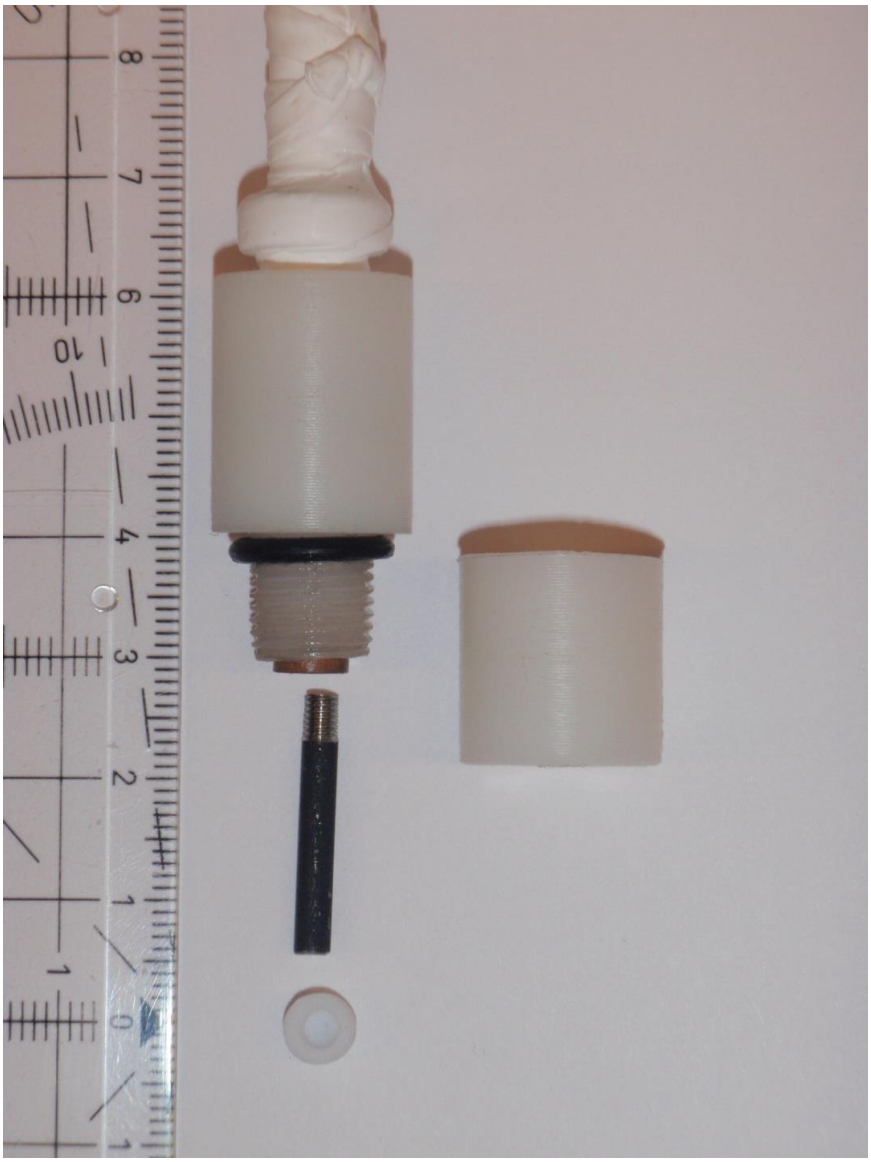

Figure 21. Sample and sample holder.

6.2 Test equipment

The experiments were carried out in three electrode cells. The working electrode was the DSA anode, the counter electrode was platinum plate or ring, and the reference electrode was saturated calomel electrode (SCE) type Radiometer 401. Potential values in the experimental part are given in SCE scale. To protect the reference electrode an electrolyte

bridge type B 521 with porous platinum frit were used. Reference electrodes were always outside the measurement cell at room temperature. In activity measurements and in polarization curve measurements a small Metrohm 6.1418.250 titration vessel with Metrohm 6.1414.010 lid was used. The cell volume was 200 ml and the temperature was controlled by thermostated water bath. Figure 22 show the test arrangement with the small cell. For long-term galvanostatic anode corrosion tests a large 5 liter cell was used. The temperature of large cell was controlled by heating plate. The purpose of a large solution volume was to maintain constant electrolyte composition during the test. With this combination the depositing of metal can be decreased and no significant change in the electrolyte was expected. These measurements were carried out in the cell that can be seen in Figure 23.

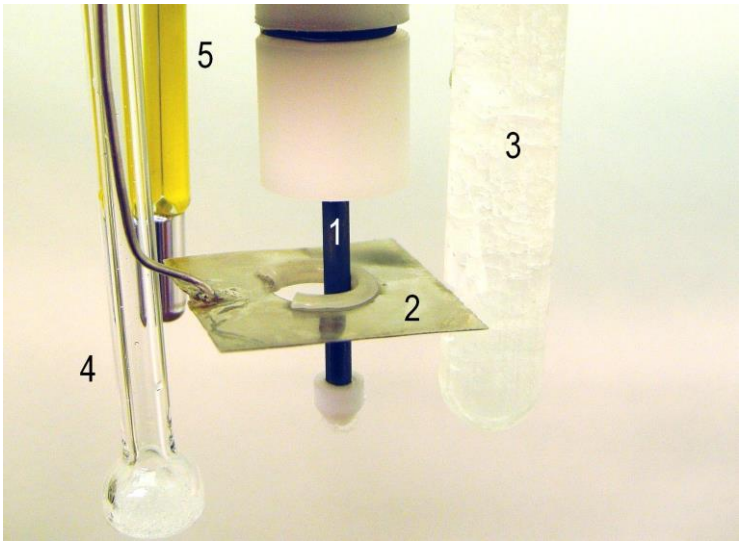

Figure 22. Three electrode cell for activity measurements and polarization curves: 1 – working DSA electrode, 2 – Pt counter electrode, 3 – SCE reference electrode in bridge, 4 – gas bubbling tube, 5 – thermometer.

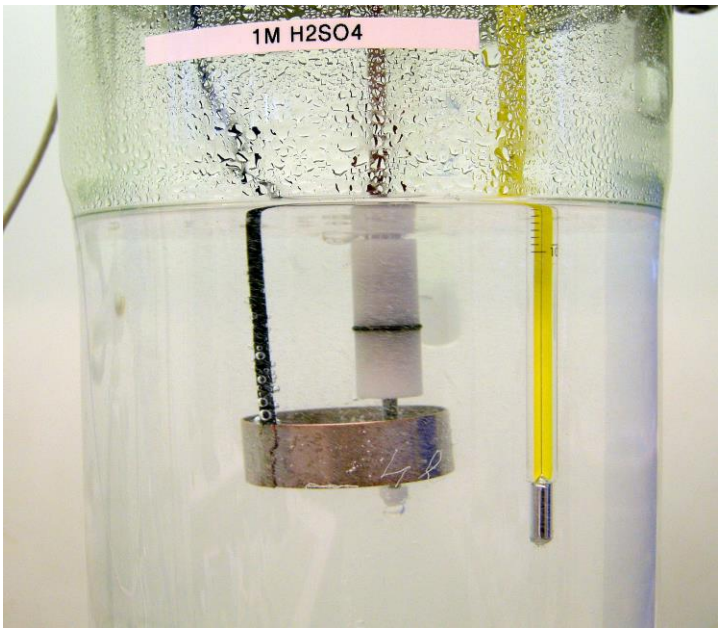

Figure 23. Installation for long-term galvanostatic anode corrosion tests in large 5 liter vessel.

Activity measurements and polarization curves were done using AMESTEK VersaSTAT-4 potentiostat with VersaStudio software and long-term galvanostatic anode corrosion tests were done using AUTOLAB potentiostat with GPES software and ACM Instruments GillAC potentiostat with ACM Instruments software version 5.

SEM images were taken with Hitachi TM-1000 Scanning Electron Microscope.

6.3 Test procedures

The effect of sulfuric acid concentration, different metal ions and different temperatures to polarization behavior of the anode were examined by polarization curves. The wear and destruction of anode were experiment by long-term galvanostatic corrosion tests. The changes in anode activity were examined by cyclic voltammetry and electrochemical impedance spectroscopy.

6.3.1 Polarization curves

Anodic polarization curves were measured in sulfuric acid solution without metal ions using H_2SO_4 concentration 50, 100, 150 and 200 g/l. With a constant acid concentration 100 g/l the effect of metal ions was tested using 20, 40 and 60 g/l of Cu^{2+}, Zn^{2+}, Ni^{2+} or Fe^{2+}. The anodic polarization curves were measured at 30, 40, 50 and 60 °C. Anodic polarization curves were measured between 1 and 2 V vs. SCE using staircase linear scan with scan rate 0.8333 mV/s.

Measured polarization curves were corrected for IR-drop afterwards by subtracting from each measured potential value the product of R_Ω and corresponding current, equation (28).

$$\mathrm{E} = E_{measured} - I_{measured} \cdot R_\Omega \qquad (28)$$

The measured ohmic resistances were small. In sulfuric acid solutions with concentration 50-200 g/l and temperature 30-60 ºC the ohmic resistance was 0.2-0.7 Ω. The effect of compensation of the ohmic resistance is shown in Figure 24. If the curve was overcompensated when used the measure ohmic resistance value, a lower estimated value was used.

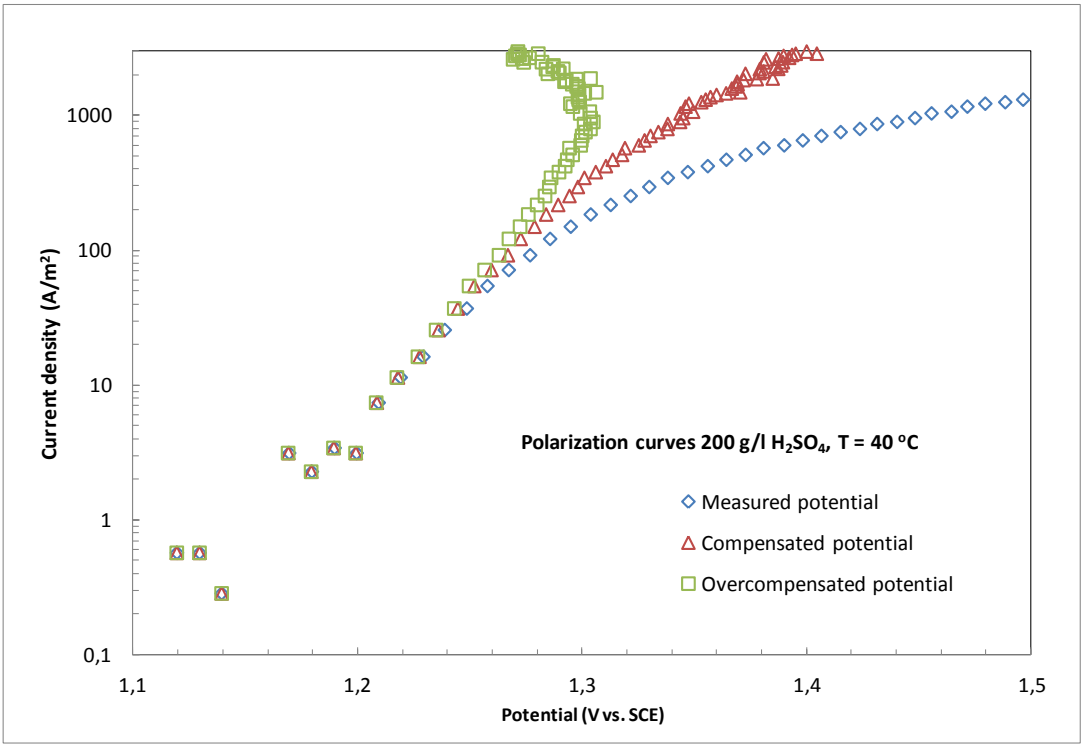

Figure 24. The effect of uncompensated and overcompensated ohmic drop. Ohmic drop was corrected to evaluate correctly the anode overpotential.

The analysis of polarization curves was done using Regression tool of Microsoft Excel 2010 data analysis package. Statistical analyses of significance of regression equations for Tafel slope, activation energy and operating potential were done using F-test and t-test.

6.3.2 Galvanostatic lifetime tests

Galvanostatic lifetime tests were made in 100 g/l sulfuric acid solution without and with metal ions. The concentration of Cu^{2+}, Zn^{2+}, Ni^{2+}, Fe^{2+} ions were 60 g/l. The starting current density was 50 mA/cm^2 and was increased by 50 mA/cm^2 per day until the anode passivated or the current density was at the maximum value that potentiostat could give. In Fe^{2+} containing solution the starting current density was 300 mA/cm^2 and was increased by 100 mA/cm^2 per day until the anode passivated or the current density was at the maximum value that potentiostat could give.

The result from galvanostatic test was the amount of electricity that is needed to passivate the anode. When knowing the amount of electricity and current density that is used in commercial process, the approximate life time of the anode in process conditions can be calculated.

6.3.3 Anode activity measurements

The anode activity experiments were made in nitrogen purged 1 M sulfuric acid solution. During the experiment the anode was polarized to 1200 mV vs SCE to facilitate oxygen evolution. The selected potential was based on polarization curves. The amplitude of the excitation signal was 10 mV RMS and the frequency range was 10 mHz – 100 kHz. Cyclic voltammetry was used to determine the voltammetric charge, which is associated with the redox reactions of active sites on the anode surface and is a measure of electrochemically active surface area [Savinell et. al. 1990]. Cyclic voltammograms were measured in the potential range -0.35…+0.6 V vs. SCE using scan rates 10, 100, 500 and 1000 mV/s. Potential and current density values were recorded at 0.95 mV intervals.

7 RESULTS

The experimental results include analysis of polarization curves to find out factors that affect anode operating potential, long-term galvanostatic tests to measure anode operating time and anode activity measurements to estimate anode damage mechanisms.

7.1 Polarization curves

The analysis of polarization curves included determination of the effects of sulfuric acid concentration, metal ion concentration and temperature on the anode operating potential. Possible changes in the reaction mechanism in the low current density and high current density ranges were estimated by calculating Tafel slopes and activation energies.

7.1.1 Sulfuric acid

Polarization curves measured in 50 g/l to 200 g/l sulfuric acid showed two linear ranges. The change from low Tafel slope range to high Tafel slope range happened at approximately current densities 200-300 A/m^2. The anode potential at constant current density decreased with increasing temperature or the current density at constant potential increased with increasing temperature as shown in Figure 25. The same tendency was seen in all tested sulfuric acid concentrations. The effect of acid concentration at constant temperature is shown in Figure 26. The anode potential at constant current density increased with increasing acid concentration or the current density at constant potential decreased with increasing acid concentration. The same tendency was seen at all tested temperatures, but the difference between 150 g/l and 200 g/l acid concentrations was not always as clear as in Figure 30.

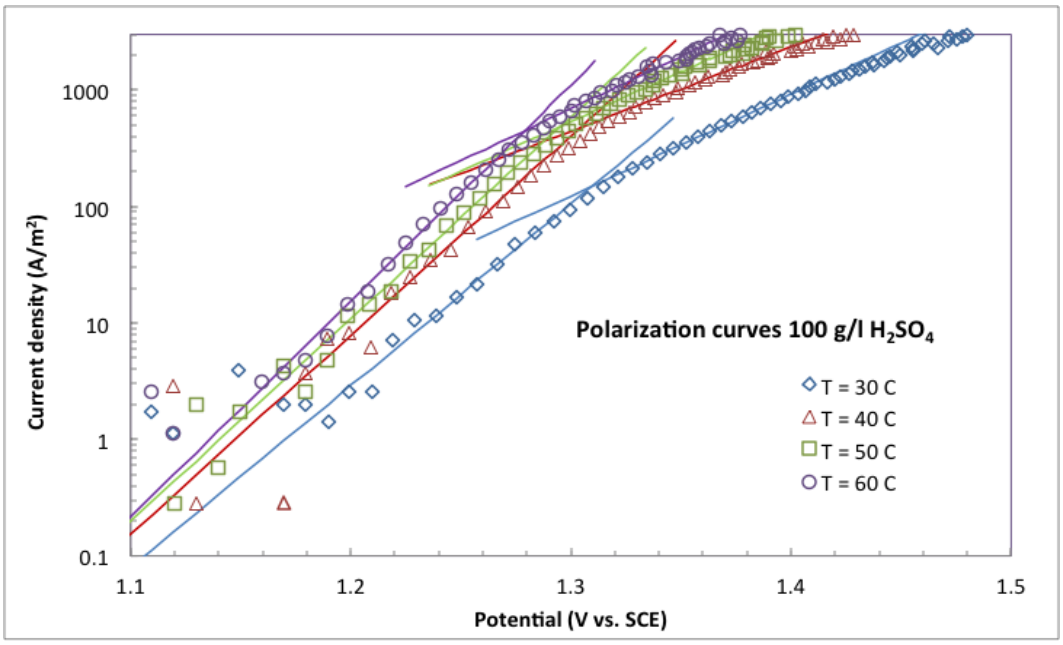

Figure 25. Polarization curves in 100 g/l H_2SO_4 including the Tafel slopes.

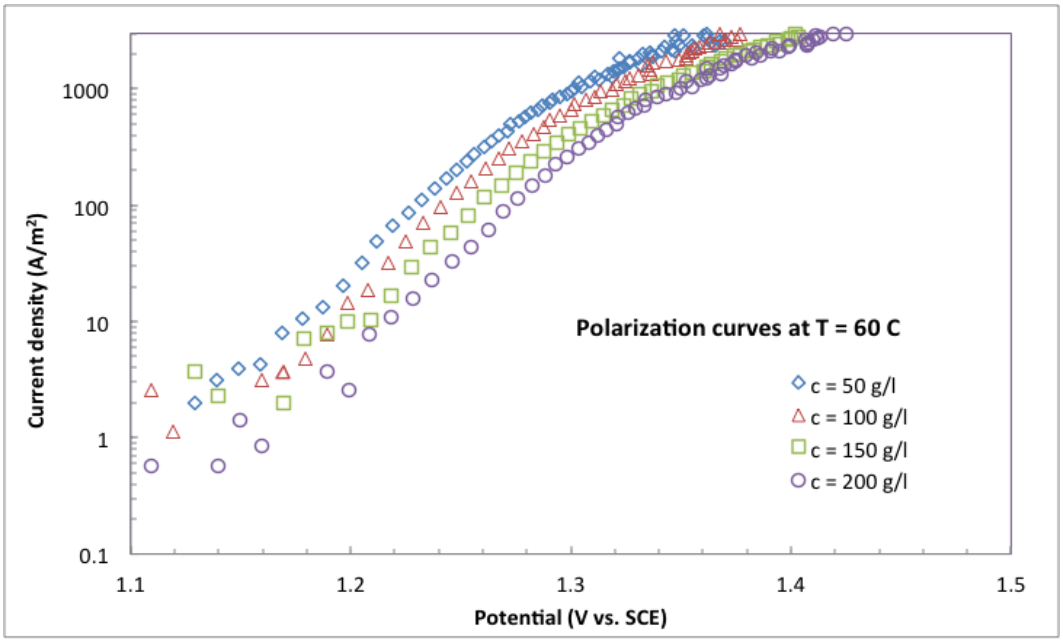

Figure 26. Polarization curves at T = 60 ºC.

Table 2 shows the calculated Tafel slopes as function of acid concentration and temperature at the low and high current density ranges. At the low current density range Tafel slope decreases with increasing temperature and acid concentration, except that the Tafel slopes in 200 g/l sulfuric acid are lower than in 150 g/l acid. At the high current density range the Tafel slope values have maximum at T = 40 ºC and the slope values decrease with increasing acid concentration. The Tafel slope at low current density range was 48-66 mV with average value 56 mV. The Tafel slope at high current density range was 90-152 mV with average value 115 mV.

Table 2. Calculated Tafel slopes in sulfuric acid.

Temperature (°C)	Concentration (g/l)	Tafel slope (mV), low current density range	Tafel slope (mV), high current density range
30	50	61	129
40	50	49	152
50	50	51	137
60	50	54	113
30	100	64	114
40	100	58	138
50	100	58	117
60	100	54	112
30	150	66	116
40	150	64	112
50	150	60	97
60	150	49	90
30	200	49	95
40	200	51	97
50	200	48	120
60	200	53	91

Table 3 shows the calculated activation energies at low and high current density range. At low current density range the calculated activation energies are slightly over 20 kJ/mol. This means that the reaction on the anode is controlled by both mass transfer and charge transfer. At high current density range the calculated activation energies at c = 50 g/l and c = 200 g/l are also in the range between 20 to 40 kJ/mol and the reaction is controlled by

mass transfer and charge transfer. At concentrations c = 100 g/l and c = 150 g/l calculated activation energies are less than 20 kJ/mol, which means that the reaction is controlled by mass transfer.

Table 3. Calculated activation energies at low and high current density range.

Potential (V)	Concentration (g/l)	Activation energy (kJ/mol)
1.25	50	26.2
1.25	100	24.0
1.25	150	23.3
1.25	200	25.8
1.35	50	23.3
1.35	100	10.7
1.35	150	13.9
1.35	200	31.1

Table 4 shows the calculated potential changes as function of acid concentration. The effect of acid concentration is between 0.01 and 0.14 mV/g/l. It seems that acid concentration has not significant effect to anode's potential.

Table 4. Calculated potential change as function of acid concentration.

Temperature (^{o}C)	Current density (A/m^{2})	ΔE/Δc (mV/g/l)
30	10	0.09
40	10	0.14
50	10	0.13
60	10	0.07
30	100	0.10
40	100	0.13
50	100	0.10
60	100	0.10
30	500	0.01
40	500	0.07
50	500	0.03
60	500	0.06

7.1.2 Copper containing electrolytes

Polarization curves measured in 100 g/l sulfuric acid containing 20 to 60 g/l copper ions showed two linear ranges. The change from low Tafel slope range to high Tafel slope range happened at current densities 80-200 A/m^2 depending on the temperature. The anode potential at constant current density decreased with increasing temperature or the current density at constant potential increased with increasing temperature as shown in Figure 27. The same tendency was seen in all tested copper ion concentrations. The effect of copper ion concentration at constant temperature is shown in Figure 28. The anode potential at constant current density increased with copper ion concentration or the current density at constant potential decreased with increasing copper ion concentration. The tendency was not very strong and at some temperatures it was not continuous.

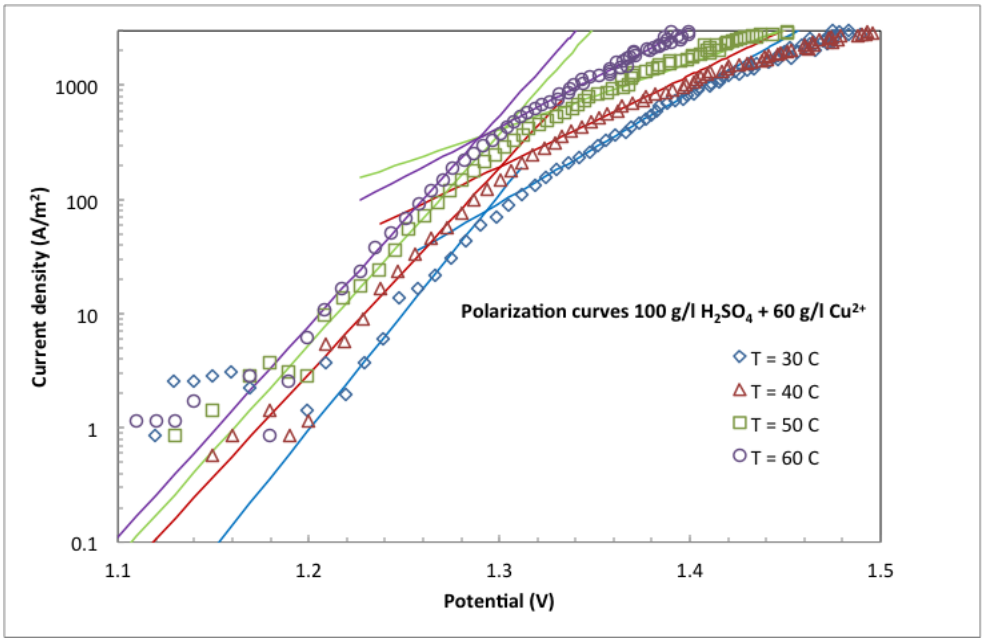

Figure 27. Polarization curves with Tafel slopes in 100 g/l H_2SO_4 with 60 g/l Cu^{2+} at different temperatures.

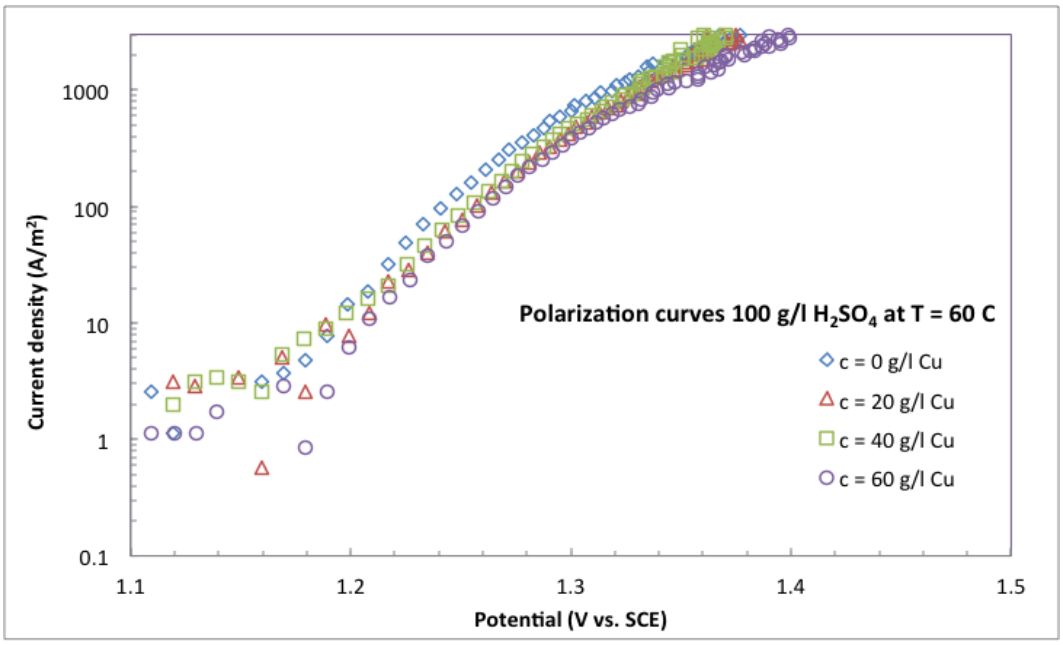

Figure 28. Polarization curves in 100 g/l H_2SO_4 with different Cu^{2+} concentrations at T = 60 ºC.

Table 5 shows Tafel slopes as function of temperature and copper concentration at low and high current density ranges. At the low current density range Tafel slope increases with increasing temperature up to 50 ºC and decreases with increasing copper ion concentration. At the high current density range the Tafel slope values decrease with increasing temperature and increase with increasing copper ion concentration. The Tafel slope in copper-containing solutions at low current density range was 48-66 mV with average value 55 mV. At the high current density range, excluding the outlier in test at T = 50 ºC and Cu^{2+} = 60 g/l, the Tafel slope was 71-103 mV with average value 85 mV. The Tafel slope values were same than in sulfuric acid electrolytes at the low current density range but clearly lower at the high current density range.

Table 5. Calculated Tafel slopes in 100 g/l sulfuric acid with 0-60 g/l copper ions.

Temperature (°C)	Concentration (g/l)	Tafel slope (mV), low current density range	Tafel slope (mV), high current density range
30	0	64	114
40	0	58	138
50	0	58	117
60	0	54	112
30	20	59	93
40	20	54	82
50	20	56	71
60	20	56	72
30	40	51	99
40	40	62	84
50	40	66	80
60	40	52	74
30	60	48	103
40	60	53	86
50	60	51	129
60	60	52	84

Table 6 shows the calculated activation energies at low and high current density range. At both low and high current density range the calculated activation energies are slightly over 20 kJ/mol. This means that the reaction in the anode is controlled by both mass transfer and charge transfer.

Table 6. Calculated activation energies at low and high current density range.

Potential (V)	Concentration (g/l)	Activation energy (kJ/mol)
1.25	20	21.2
1.25	60	21.8
1.35	20	24.6
1.35	60	26.3

Table 7 shows the calculated potential changes as function of metal concentration. The absolute values of effect of metal concentration are between 0.01 and 1.34 mV/g/l. It seems that metal concentration has not significant effect to anode's potential at generally. At T = 40 ^{o}C and i = 500 A/m^2 there is a stronger effect, but this is more likely an exception.

Table 7. Calculated potential change as function of metal concentration.

Temperature (^{o}C)	Current density (A/m^2)	ΔE/Δc (mV/g/l)
30	10	0.10
40	10	0.35
50	10	0.14
60	10	0.17
30	100	0.14
40	100	0.07
50	100	-0.04
60	100	0.06
30	500	0.27
40	500	1.34
50	500	0.04
60	500	-0.01

7.1.3 Nickel containing electrolytes

Polarization curves measured in 100 g/l sulfuric acid containing 20 to 60 g/l nickel ions showed two linear ranges. The change from low Tafel slope range to high Tafel slope range happened at current densities 80-300 A/m^2 depending on the temperature. The anode potential at constant current density decreased with increasing temperature or the current density at constant potential increased with increasing temperature as shown in Figure 29. At the highest current densities the anodes had approximately 100 mV higher polarization in nickel containing electrolytes than in sulfuric acid, especially at lower temperatures.

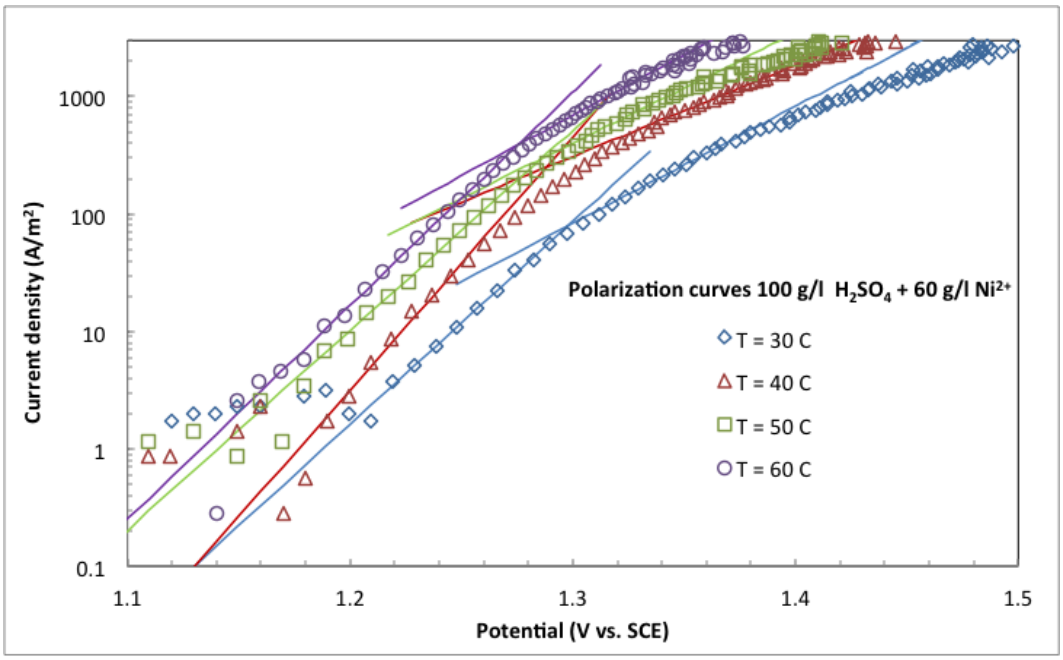

Figure 29. Polarization curves with Tafel slopes in 100 g/l H_2SO_4 with 60 g/l Ni^{2+} at different temperatures.

The effect of nickel ion concentration at constant temperature is shown in Figures 30 and 31. At low temperatures the anode potential at constant current density increased with nickel ion concentration or the current density at constant potential decreased with increasing nickel ion concentration. The tendency was not very strong and not always continuous. The lowest nickel concentration increased slightly the current density whereas higher concentration decreased when compared with sulfuric acid. At highest temperature no effect of nickel ion concentration on anode potential was seen.

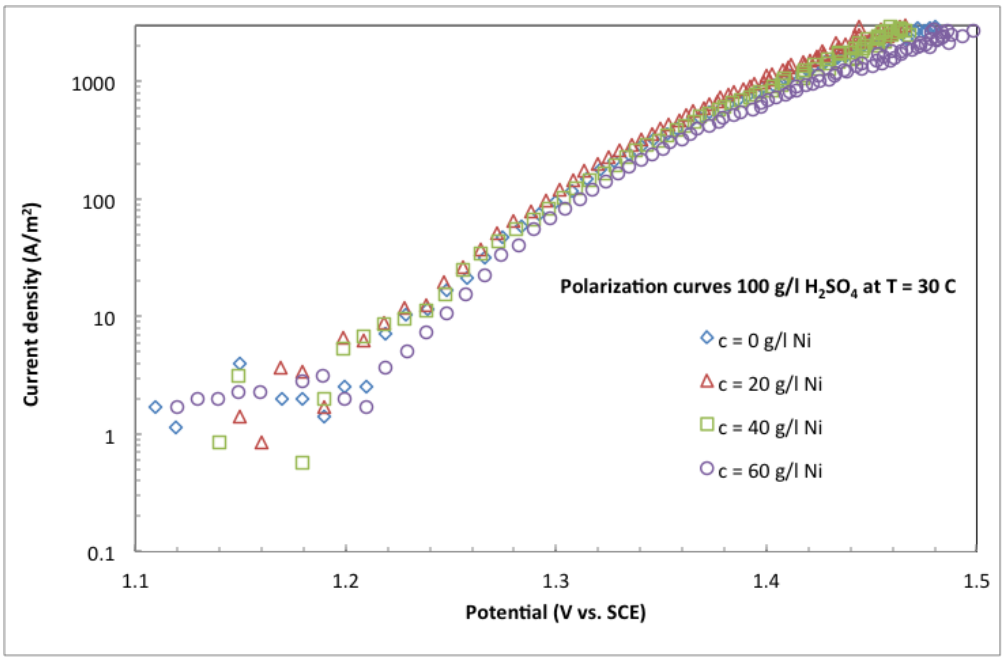

Figure 30. Polarization curves in 100 g/l H_2SO_4 with different Ni^{2+} concentrations at T = 30 ºC.

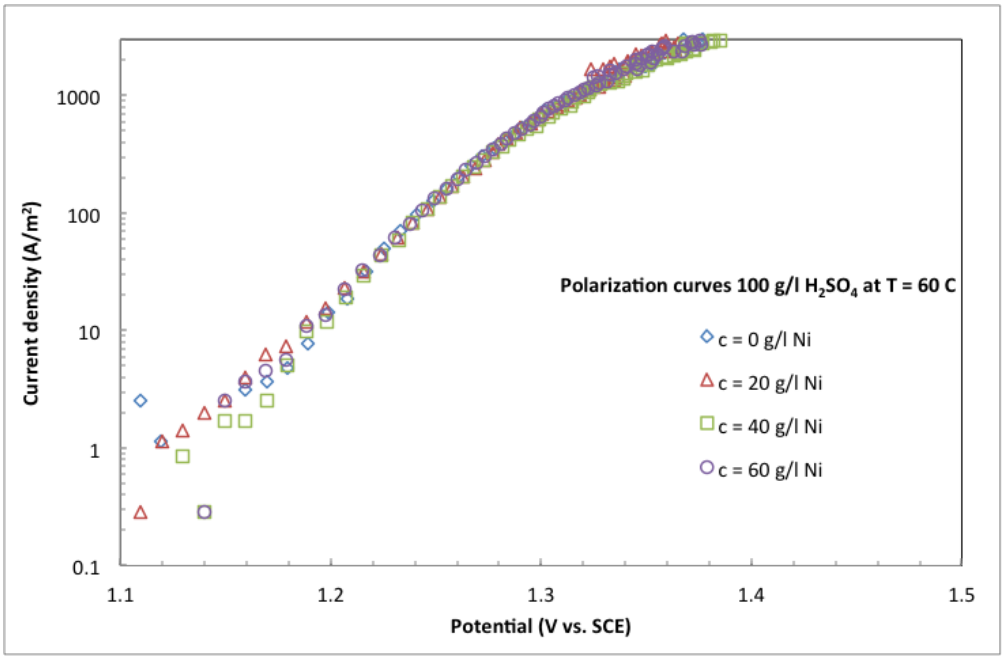

Figure 31. Polarization curves in 100 g/l H_2SO_4 with different Ni^{2+} concentrations at T = 60 ºC.

Table 8 shows Tafel slopes as function of temperature and nickel concentration at low and high current density ranges. At the low current density range Tafel slope values decreased slightly with increasing temperature and increasing nickel ion concentration. At the high current density range the Tafel slope values decreased clearly with increasing temperature but nickel ion concentration had no clear effect. At the low current density range, excluding the outlier in test at T = 30 ºC and Ni^{2+} = 40 g/l, the Tafel slope in nickel-containing solutions at low current density range was 47-59 mV with average value 54 mV. At the high current density range the Tafel slope was 63-137 mV with average value 97 mV. The Tafel slope values were same than in sulfuric acid electrolytes at the low current density range but lower at the high current density range. It must be noticed that at the high current density range the Tafel slopes were extremely scattered.

Table 8. Calculated Tafel slopes in 100 g/l sulfuric acid with 0-60 g/l nickel ions.

Temperature (^{o}C)	Concentration (g/l)	Tafel slope (mV), low current density range	Tafel slope (mV), high current density range
30	0	64	114
40	0	58	138
50	0	58	117
60	0	54	112
30	20	58	97
40	20	55	106
50	20	49	111
60	20	58	84
30	40	80	137
40	40	57	85
50	40	51	69
60	40	47	63
30	60	59	109
40	60	47	129
50	60	56	83
60	60	53	73

Table 9 shows the calculated activation energies at low and high current density range. At low current density range the calculated activation energies are slightly over 20 kJ/mol and at high current density range the activation energies are around 30 kJ/mol. This means that the reaction in the anode at both current density ranges are controlled by both mass transfer and charge transfer.

Table 9. Calculated activation energies at low and high current density range.

Potential (V)	Concentration (g/l)	Activation energy (kJ/mol)
1.25	20	21.9
1.25	60	22.0
1.35	20	27.8
1.35	60	30.9

Table 10 shows the calculated potential changes as function of metal concentration. The absolute values of effect of metal concentration are between 0.05 and 8.27 mV/g/l. It seems that metal concentration has not significant effect to anode's potential at higher current densities (i = 100 A/m^2 and i = 500 A/m^2) when T = 50 ^{o}C or higher. At T = 30 ^{o}C at all current densities it seems that there is strong correlation between metal concentration and potential. Also at T = 40 ^{o}C at all current densities and at higher temperatures at low current density (i = 10 A/m^2) there can been seen correlation between metal concentration and potential.

Table 10. Calculated potential change as function of metal concentration.

Temperature (^{o}C)	Current density (A/m^2)	ΔE/Δc (mV/g/l)
30	10	5.03
40	10	2.23
50	10	0.57
60	10	1.07
30	100	4.51
40	100	1.81
50	100	-0.10
60	100	-0.44
30	500	8.27
40	500	1.90
50	500	0.39
60	500	-0.05

7.1.4 Zinc containing electrolytes

Polarization curves measured in 100 g/l sulfuric acid containing 20 to 60 g/l zinc ions showed two linear ranges as in the measurements with copper and nickel. The change from low Tafel slope range to high Tafel slope range happened at current densities 50-300 A/m^2 depending on the temperature. The anode potential at constant current density decreased with increasing temperature or the current density at constant potential increased with increasing temperature as shown in Figure 32. At the highest current densities the anodes had approximately 100 mV higher polarization in zinc containing electrolytes than in sulfuric acid. Especially at lower temperatures the polarization was stronger than in copper or nickel containing electrolytes. The anode potential at constant current density increased with zinc ion concentration or the current density at constant potential decreased with increasing zinc ion concentration. The tendency was not very strong and it was not always continuous, Figure 33.

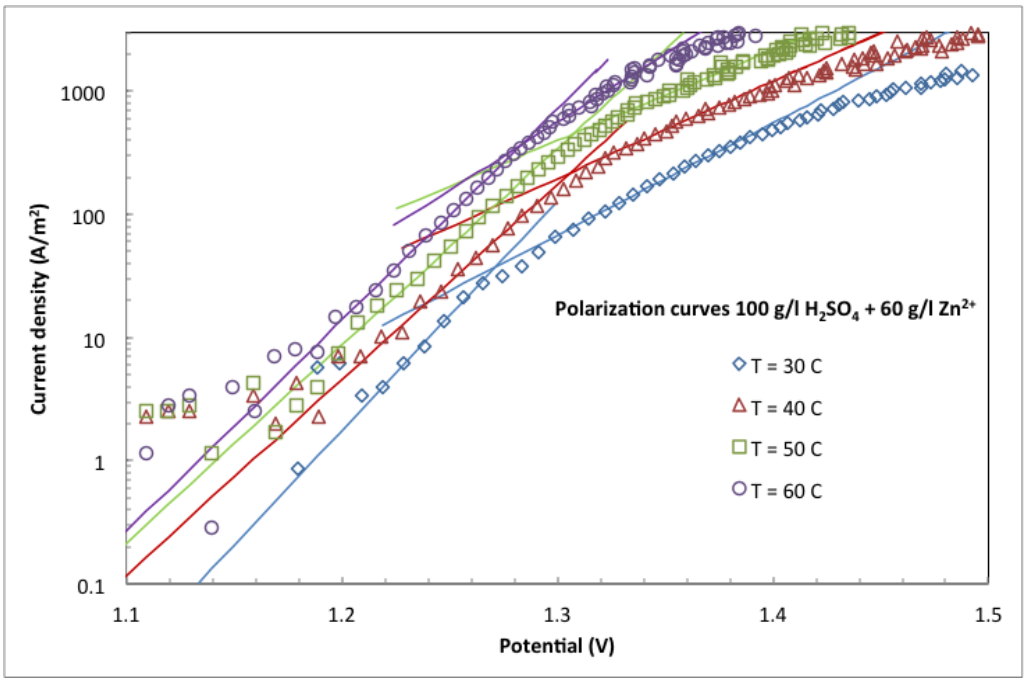

Figure 32. Polarization curves with Tafel slopes in 100 g/l H_2SO_4 with 60 g/l Zn^{2+} at different temperatures.

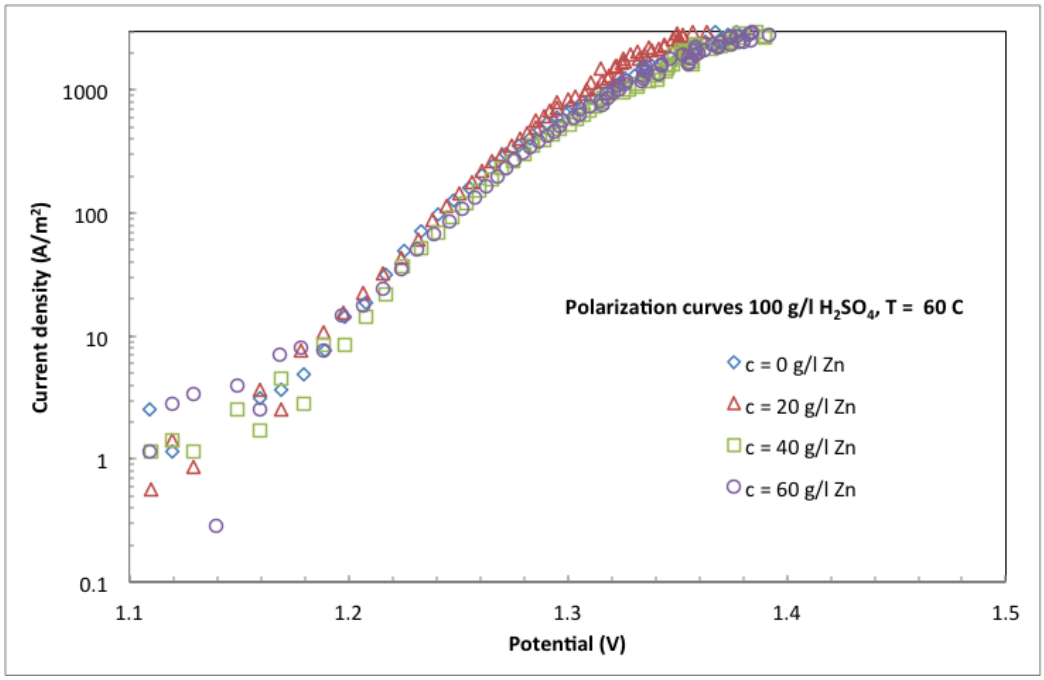

Figure 33. Polarization curves in 100 g/l H_2SO_4 with different Zn^{2+} concentrations at T = 60 ºC.

Table 11 shows Tafel slopes as function of temperature and zinc concentration at low and high current density ranges. At the low current density range Tafel slope values decreased slightly with increasing temperature and increased slightly with increasing zinc ion concentration. At the high current density neither temperature or zinc concentration had clear effect. At the low current density range the Tafel slope in nickel-containing solutions at low current density range was 49-63 mV with average value 54 mV. At the high current density range the Tafel slope was 83-147 mV with average value 111 mV. The Tafel slope values were same than in sulfuric acid electrolytes at the low current density range but lower at the high current density range. It must be noticed that as with the nickel electrolytes at the high current density range the Tafel slopes were extremely scattered.

Table 11. Calculated Tafel slopes in 100 g/l sulfuric acid with 0-60 g/l zinc ions.

Temperature (^{o}C)	Concentration (g/l)	Tafel slope (mV), low current density range	Tafel slope (mV), high current density range
30	0	64	114
40	0	58	138
50	0	58	117
60	0	54	112
30	20	53	123
40	20	51	83
50	20	49	120
60	20	53	113
30	40	51	111
40	40	53	147
50	40	51	89
60	40	49	105
30	60	54	110
40	60	63	127
50	60	62	136
60	60	58	91

Table 12 shows the calculated activation energies at low and high current density range. At both low and high current density range the calculated activation energies are in the range between 25 and 30 kJ/mol. This means that the reaction in the anode is controlled by both mass transfer and charge transfer.

Table 12. Calculated activation energies at low and high current density range.

Potential (V)	Concentration (g/l)	Activation energy (kJ/mol)
1.25	20	25.8
1.25	60	23.2
1.35	20	29.8
1.35	60	25.4

Table 13 shows the calculated potential changes as function of metal concentration. The absolute values of effect of metal concentration are between 0.03 and 1.02 mV/g/l. It seems that metal concentration has not significant effect to anode's potential at generally. There is some correlation between metal concentration and potential at i = 500 A/m^2, T = 30 - 50 ^{o}C and at i = 10 A/m^2, T = 60 ^{o}C, but thy can be considered as exceptions.

Table 13. Calculated potential change as function of metal concentration.

Temperature (^{o}C)	Current density (A/m2)	ΔE/Δc (mV/g/l)
30	10	0.26
40	10	0.13
50	10	0.03
60	10	0.98
30	100	0.38
40	100	0.45
50	100	0.32
60	100	0.22
30	500	0.81
40	500	1.02
50	500	0.69
60	500	0.41

7.1.5 Iron containing electrolytes

The iron containing electrolytes were expected to show different polarization behavior than sulfuric acid or sulfuric acid with copper, nickel or zinc. The ferrous ion is capable to be oxidized to ferric iron, which means that there could be two different anodic reactions proceeding on the anode surface; oxygen evolution and iron oxidation. Polarization curves measured in 100 g/l sulfuric acid containing 20 to 60 g/l ferrous ions showed first oxidation

of ferrous iron at limiting current density up to 1.2-1.3 V vs. SCE and this was followed by oxygen evolution. When the anode potential is high enough both reactions will proceed. In the oxygen evolution potential range two linear ranges were noticed as with other measurements, but this change was not always seen. Figure 34 shows polarization curves at different temperatures with 20 g/l Fe^{2+} and Figure 35 with 60 g/l Fe^{2+}. The limiting current density of ferrous ion oxidation is on the range where Tafel slopes changed in iron-free solutions. The change in Tafel slope seen in Figure 34 with 20 g/l ferrous ions is at much higher current densities than in other tested electrolytes. The same tendencies were seen as with iron-free electrolytes. The anode potential at constant current density decreased with increasing temperature or the current density at constant potential increased with increasing temperature

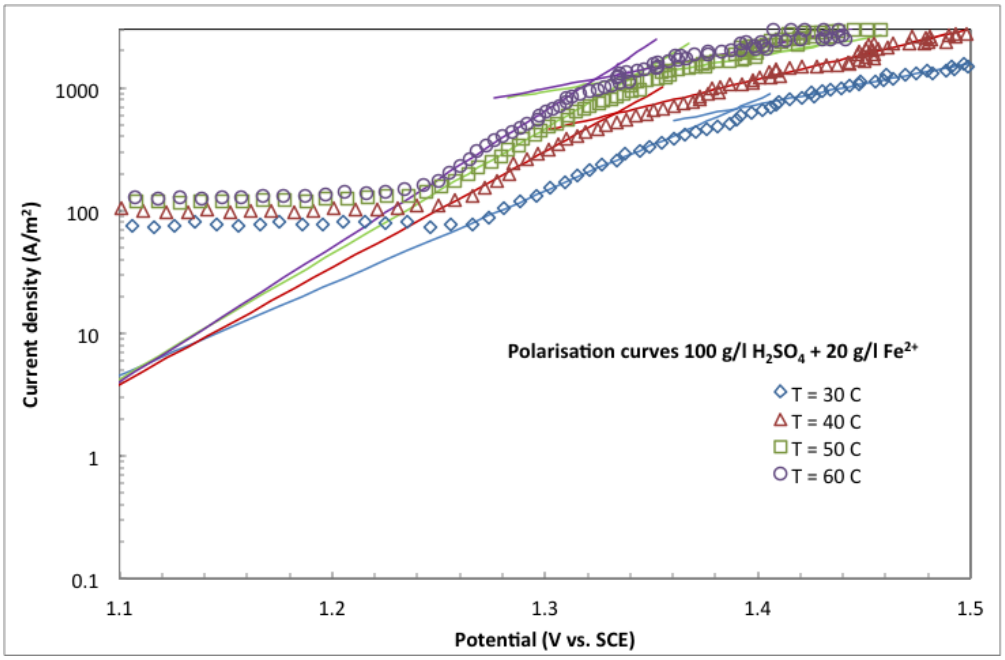

Figure 34. Polarization curves with Tafel slopes in 100 g/l H_2SO_4 with 20 g/l Fe^{2+} at different temperatures.

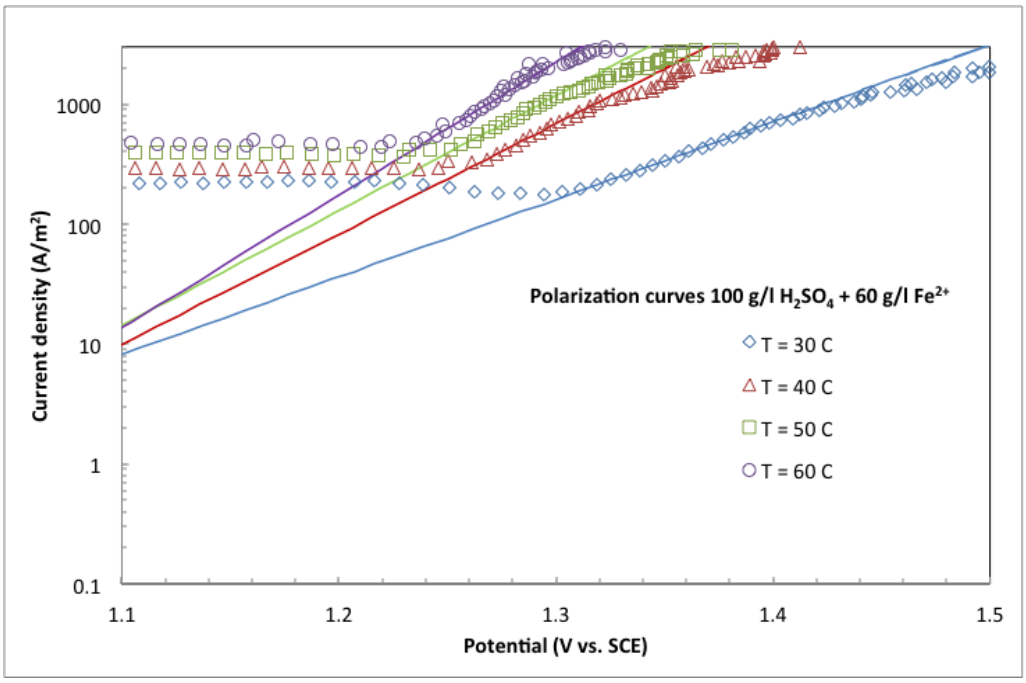

Figure 35. Polarization curves with Tafel slopes in 100 g/l H_2SO_4 with 60 g/l Fe^{2+} at different temperatures.

Figure 36 shows the effect of ferrous ion on polarization curves. Increasing the ferrous ion concentration increases current density at constant potential. This effect is seen both on the ferrous iron limiting current density range and oxygen evolution range. On the oxygen evolution range increase in ferrous ion concentration decreases operating potential. This effect is opposite when comparing with the effect of other studied metals.

Table 14 shows analysis of Tafel slopes. The analysis was done only for one current density range. In this analysis it should be noticed that the current density range for iron-free sulfuric acid is the higher one. The lower current density range was overlapped by the high limiting current density of ferrous ion oxidation. The current density range for iron-containing electrolytes was single one or the lower one in case two ranges were seen. The Tafel slope in iron containing electrolytes was 90-155 mV with average value 112 mV. The Tafel slope values in iron-containing electrolytes were same than in sulfuric acid electrolytes without iron.

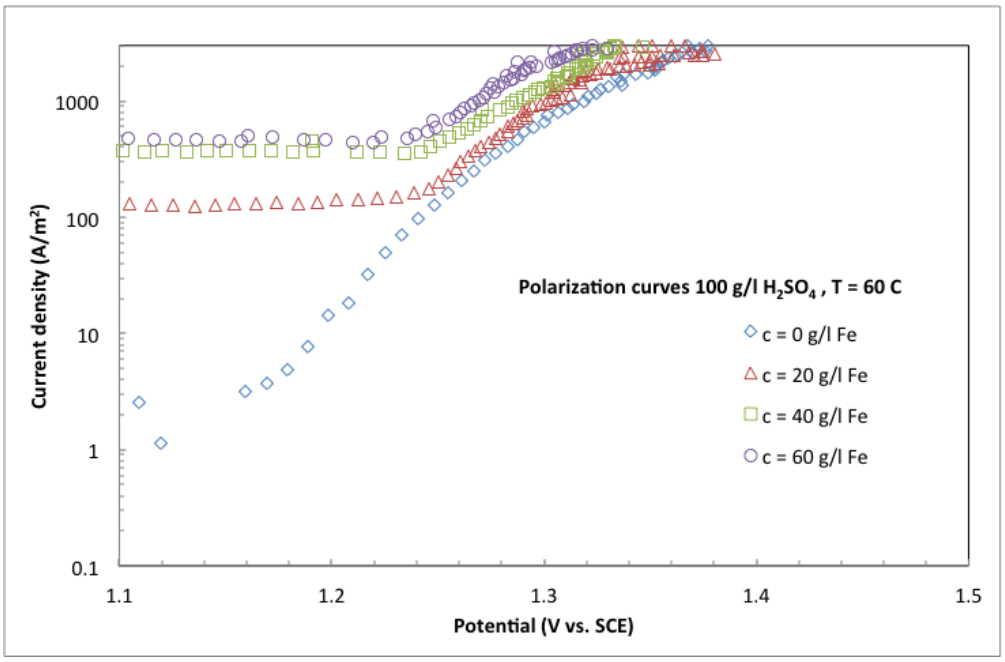

Figure 36. Polarization curves in 100 g/l H_2SO_4 with different Fe^{2+} concentrations at T = 60 ºC.

Table 14. Calculated Tafel slopes in 100 g/l sulfuric acid with 0-60 g/l ferrous ions.

Temperature (°C)	Concentration (g/l)	Tafel slope (mV)
30	0	114
40	0	138
50	0	117
60	0	112
30	20	133
40	20	105
50	20	98
60	20	90
30	40	136
40	40	112
50	40	109
60	40	103
30	60	155
40	60	109
50	60	104
60	60	91

Table 15 shows the calculated activation energies at low and high current density range. At low current density range the calculated activation energies are less than 10 kJ/mol. This means that the reaction in the anode is controlled by mass transfer. At high current density range the calculated activation energy at c = 20 g/l is 18.4, which means that the reaction is also controlled by mass transfer. At higher metal concentrations at high current density range the activation energies are over 20 kJ/mol and the reaction is controlled by mass transfer and charge transfer.

Table 15. Calculated activation energies at low and high current density range.

Potential (V)	Concentration (g/l)	Activation energy (kJ/mol)
1.2	20	6.7
1.2	40	9.4
1.2	60	8.5
1.35	20	18.4
1.35	40	24.8
1.35	60	28.2

Table 16 shows the calculated potential changes as function of metal concentration. The absolute values of effect of metal concentration are between 0.15 and 1.60 mV/g/l. It seems that metal concentration has not significant effect to anode's potential at T = 30 °C. At higher temperatures increasing iron concentration decreases operating potential.

Table 16. Calculated potential change as function of metal concentration.

Temperature (°C)	Current density (A/m^2)	ΔE/Δc (mV/g/l)
30	500	-0.15
40	500	-1.09
50	500	-1.08
60	500	-1.39
30	1000	-0.19
40	1000	-1.60
50	1000	-1.22
60	1000	-1.47

7.2 Galvanostatic tests

Galvanostatic lifetime tests were done by stepwise increase of current density and monitoring the time to sudden increase of anode potential that indicates passivation. However, none of the samples passivated during the tests. The tests were started using current densities typical for electrowinning. The maximum current densities were 10-50 higher than these. The test times were from 164 to 749 hours. The analysis of galvanostatic test included calculation of total amount of electricity during the test and dividing that to the area of the anode sample.

Figure 37 shows the amount of electricity consumed during the test as function of time in 100 g/l sulfuric acid solution. The stepwise increase in charge cumulation rate is because of increases in testing current density. Figure 38 shows the increase of potential during the same galvanostatic test. There are no signs of passivation.

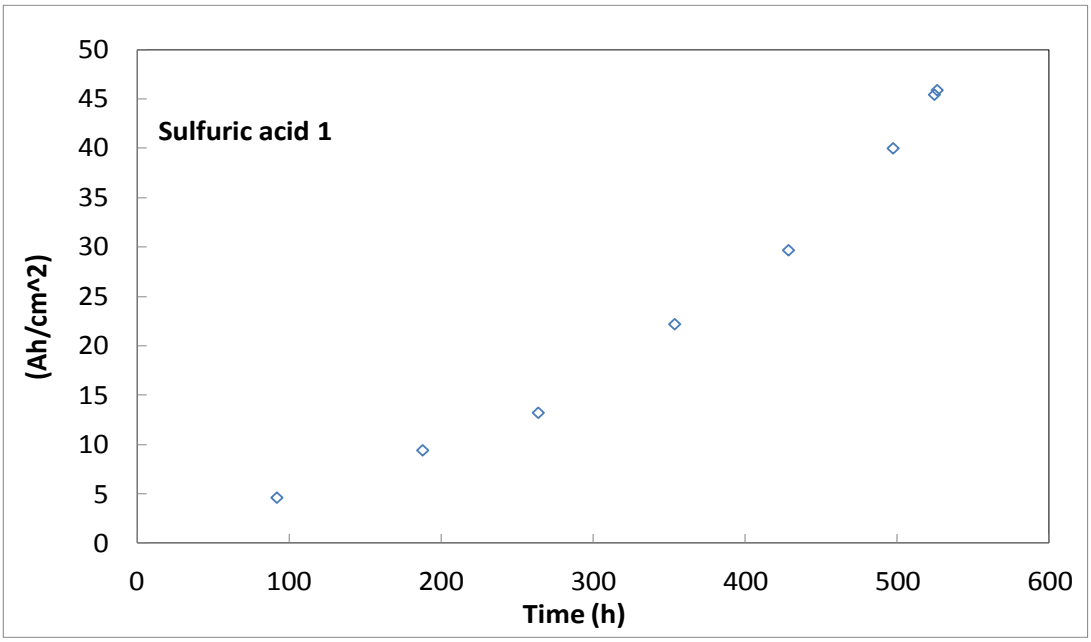

Figure 37. Charge per surface area vs. time in 100 g/l H_2SO_4 at T = 60 ^oC.

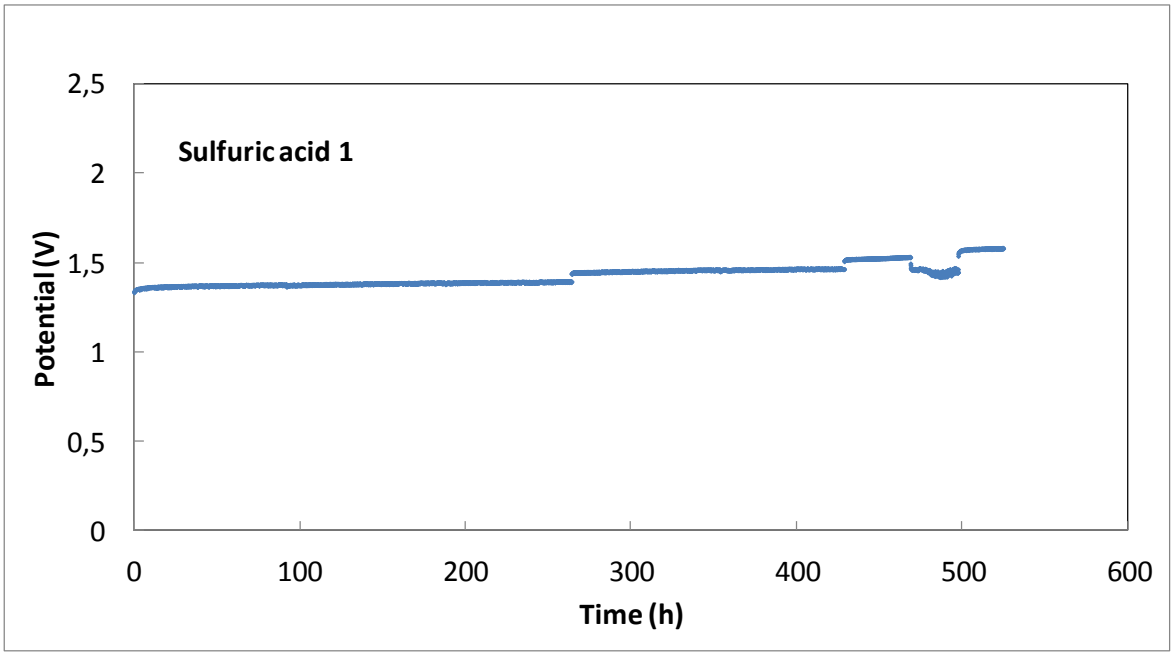

Figure 38. Anode potential vs. time in 100 g/l H_2SO_4 at T = 60 °C.

Figure 39 shows the amount of electricity that has passed during the test as function of the time in sulfuric acid solution with 60 g/l Cu^{2+}. When comparing Figures 37 and 39 it is important to notice that the tests were made by different potentiostats. In sulfuric acid test were used Gill AC potentiostat and in sulfuric acid with 60 g/l Cu^{2+} test were made by AUTOLAB potentiostat. From the results of the galvanostatic test were seen clearly that the tests, which were made by using Gill AC potentiostat were notably shorter and the amount of the electricity that gone through the anode was significantly lower. Figure 40 shows from the potential increase with time in the same galvanostatic test. Potential drops after 200 hours and before 400 hours shows that there was short circuit. Missing data points before the first short circuit is caused by re-booting of the computer and because of that the data from one test were lost. In calculations has been used estimation of the time that test was running since the used current density was known.

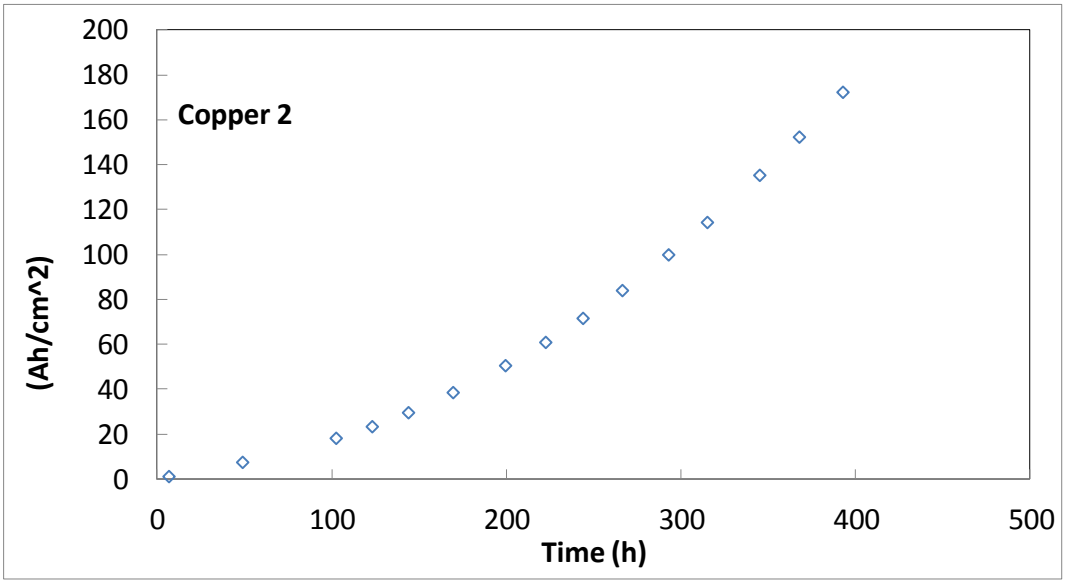

Figure 39. Charge per surface area vs. time in 100 g/l H_2SO_4 with 60 g/l Cu^{2+} at T = 60 °C.

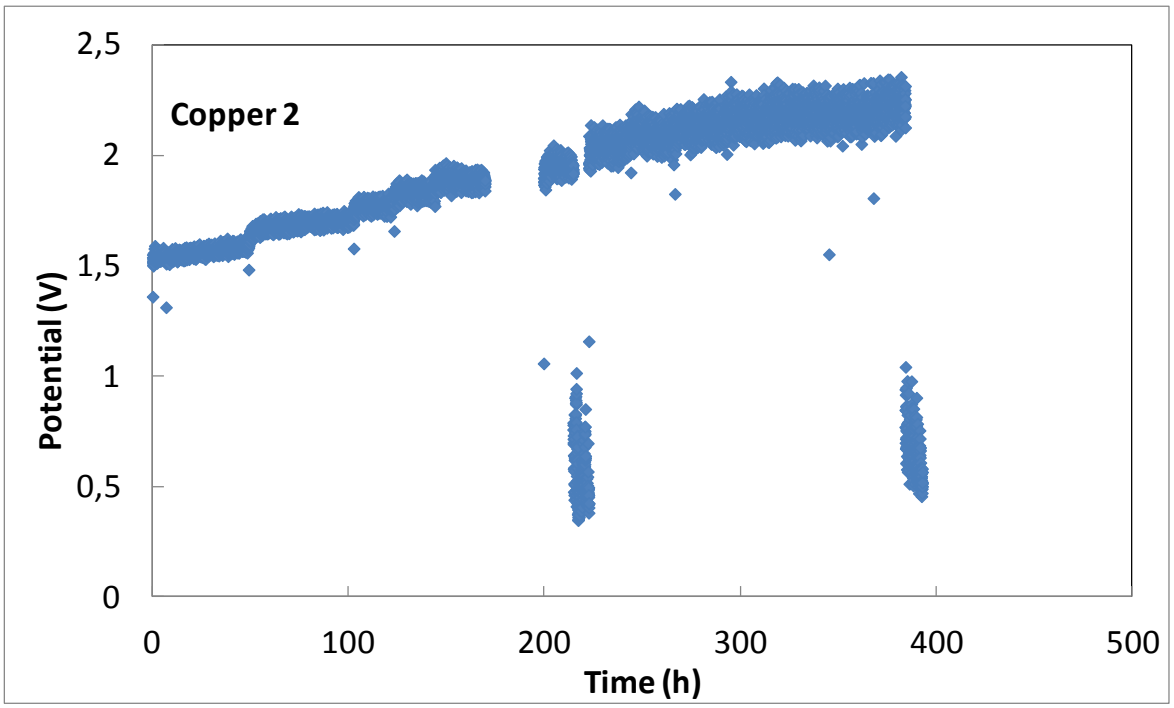

Figure 40. Potential vs. time in 100 g/l H_2SO_4 with 60 g/l Cu^{2+} at T = 60 °C.

Table 17 shows a summary of all galvanostatic lifetime tests. Sulfuric acid 1 and 2 and Copper 1 and Iron test were made by using Gill AC potentiostat and other tests were made by using the AUTOLAB potentiostat.

Table 17. Summary of galvanostatic tests.

Experiment	Time (h)	i_{max} (mA/cm^2)	Q (Ah)	Q/A (Ah/cm^2)
Sulfuric acid 1	526.6	250	99.1	45.9
Sulfuric acid 2	165.0	200	35.0	16.2
Copper 1	164.0	250	58.6	27.1
Copper 1	393.0	800	118.8	172.2
Nickel	633.9	1250	298.4	432.5
Zink 1	628.9	400	248.9	115.2
Zink 2	749.1	500	624.6	289.1
Iron	218.7	1000	98.9	143.3

7.3 Anode activity measurements

Anode activities were measured using cyclic voltammetry and electrochemical impedance spectroscopy. The charges spent during cyclic voltammograms were integrated and the charge spent on easily accessible surface sites and charge spent on all sites were extrapolated using equations (24) and (25) as shown in Chapter 5.1. Figures 41 and 42 show activity measurements before and after sulfuric acid tests number 1. Figures 43 and 44 show activity measurements before and after galvanostatic test number 1 in sulfuric acid with copper ions. The decrease of current densities indicates loss of anode activity.

EIS spectrum in Figure 45 show impedance changes during test number 2 in sulfuric acid with zinc ions. The Figure 46 shows the same changes in the test number 1 in sulfuric acid with copper ions. In both test the charge transfer resistance seen at the lowest frequencies has increased indicating loss of activity. The ohmic resistance seen at the highest frequencies has not changed. The capacitive region seen as the sloped area in the spectrum is in the same frequency range indicating that surface area of the sample has not changed.

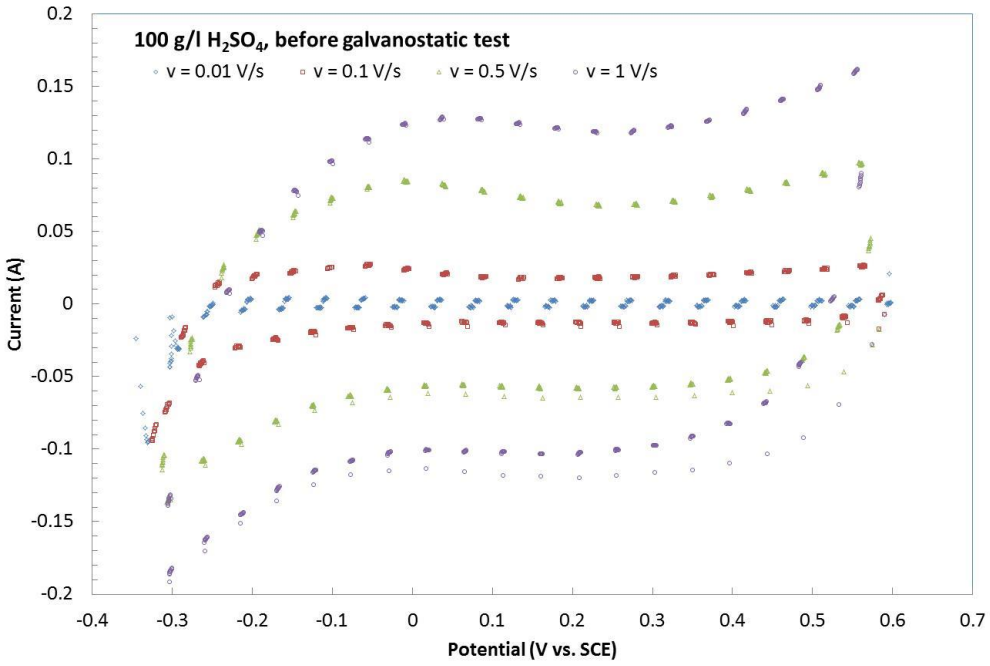

Figure 41. Cyclic voltammograms before galvanostatic testing in 100 g/l H_2SO_4.

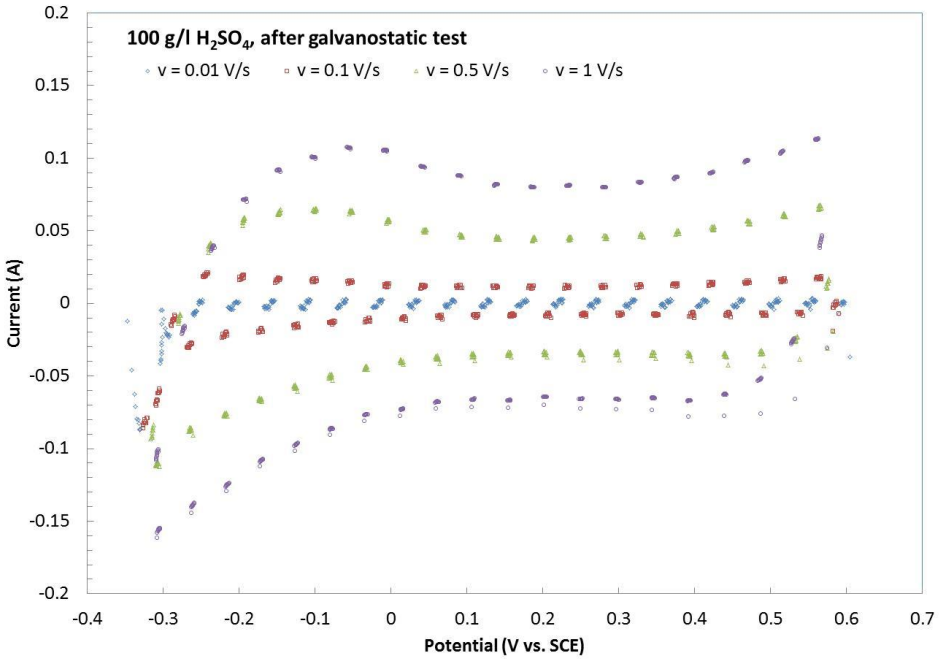

Figure 42. Cyclic voltammograms after galvanostatic testing in 100 g/l H_2SO_4.

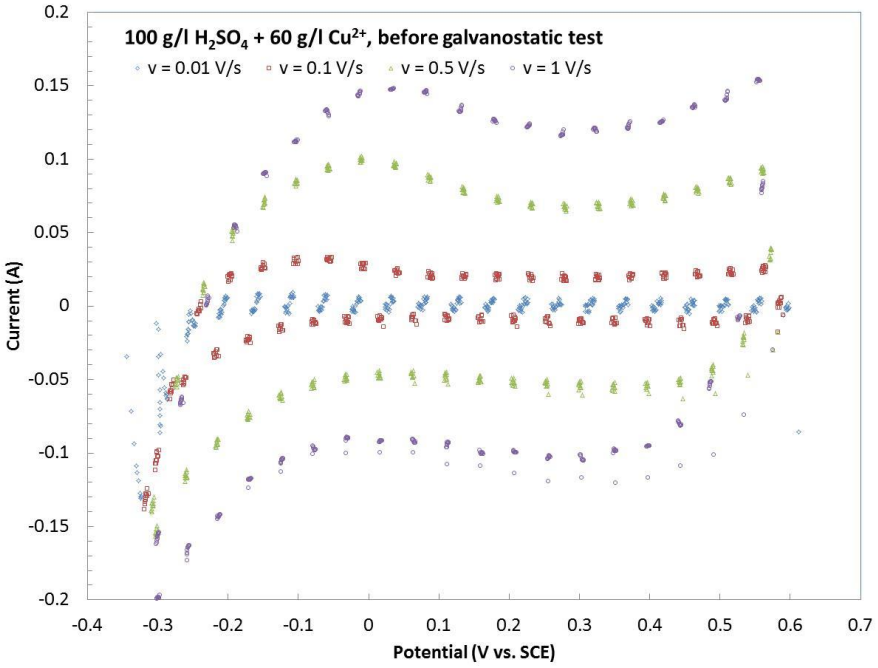

Figure 43. Cyclic voltammograms before galvanostatic testing in 100 g/l H_2SO_4 + 60 g/l Cu^{2+}.

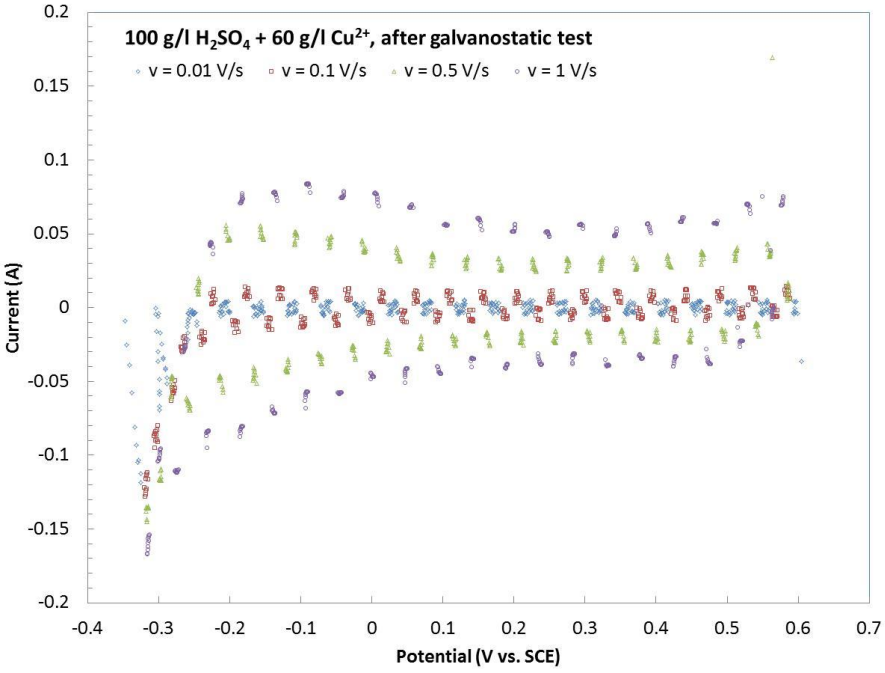

Figure 44. Cyclic voltammograms after galvanostatic testing in 100 g/l H_2SO_4 + 60 g/l Cu^{2+}.

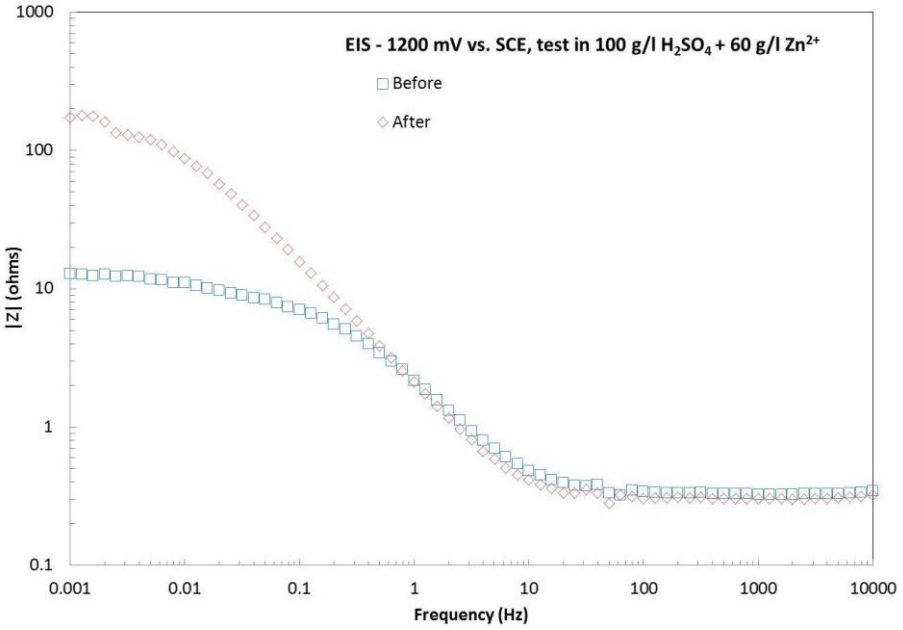

Figure 45. EIS before and after galvanostatic test in 100 g/l H_2SO_4 + 60 g/l Zn^{2+}.

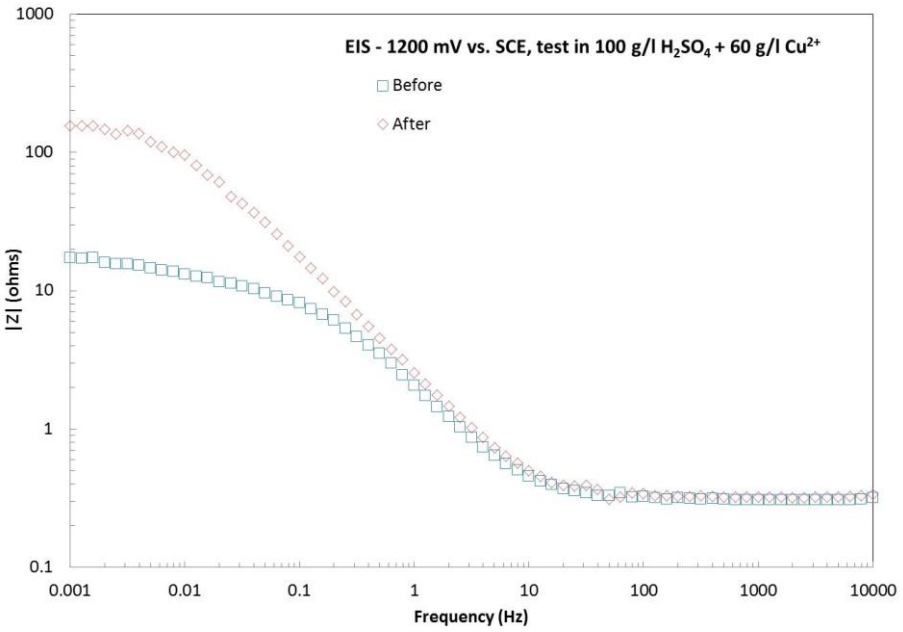

Figure 46. EIS before and after galvanostatic test in 100 g/l H_2SO_4 + 60 g/l Cu^{2+}.

The changes seen in anode activity before and after the galvanostatic tests are summarized in Table 18. Table 18 lists test description, surface and total charge before and after the test and charge transfer resistance before and after the test.

Table 18. Changes in anode surface charge, total charge and polarization resistance during galvanostatic tests.

Test	q(surface) (mC/cm^2)		q(total) (mC/cm2)		Rp (ohm*cm^2)	
	Before	After	Before	After	Before	After
100 g/l H_2SO_4, test 1	47.1	33.1	613.8	380.6	36.7	34.9
100 g/l H_2SO_4, test 2	63.3	51.6	762.5	643.6	192.2	53.0
100 g/l H_2SO_4 + 60 g/l Cu^{2+}, test 1	13.9	4.1	726.9	401.6	36.7	336
100 g/l H_2SO_4 + 60 g/l Cu^{2+}, test 2	42.2	3.1	1479.0	783.4	100.0	317.0
100 g/l H_2SO_4 + 60 g/l Zn^{2+}, test 1	38.0	1.9	889.5	429.6	49.4	240.0
100 g/l H_2SO_4 + 60 g/l Zn^{2+}, test 2	51.9	20.4	312.1	274.7	27.2	374.0
100 g/l H_2SO_4 + 60 g/l Ni^{2+}	57.7	13.4	762.2	401.4	84.7	123.0
100 g/l H_2SO_4 + 60 g/l Fe^{2+}	46.5	33.0	409.6	349.9	113.0	104.0

The results in Table 18 show clearly that anode is consumed when tested in copper or zinc containing electrolytes. This is seen as decrease in surface charge and total charge and increase in polarization resistance. Test in nickel containing electrolyte indicated same tendencies but in somewhat smaller scale. Test in iron containing electrolyte showed decrease of both charges but also small decrease of polarization resistance. These conflicting results do not allow conclusions of anode consumption in iron containing electrolytes. The same tendency as with iron was seen in sulfuric acid without metal ions. The large decrease of polarization resistance in sulfuric acid test number 2 is certainly an error.

The changes in sulfuric acid electrolytes indicate loss of the surface charge by 20-30% and loss of total charge by 15-40%. The changes of polarization resistance in sulfuric acid are not showing increase, but the decrease is not easily explained as it does not fit to the general wear model. The changes in copper-containing electrolytes indicate that the surface charge decreased by 70% or 93%, the total charge by 44-47 % and the polarization resistance increased by 200% or 800%. The changes in zinc-containing electrolytes indicate that the surface charge decreased by 61% or 95%, the total charge by 12% or 52% and the polarization resistance increased by 400% or 1200%. The changes in nickel-containing

electrolyte showed decrease of surface charge by 77%, decrease of total charge by 47% and increase of polarization resistance by 45%. The results in iron-containing electrolyte indicate loss of surface charge by 30%, loss of total charge by 15% and small decrease in polarization resistance. The loss of anode activity in copper, zinc and nickel containing electrolytes is probably linked to loss of outermost part of the active oxide. The wear and corrosion is much stronger in these electrolytes than in sulfuric acid or iron-containing electrolyte. It is also worth to note from Table 17 that in nickel or iron containing electrolytes much higher current densities and charges were used than in copper or zinc containing electrolytes. This indicates further that the metal ion can have influence on anode corrosion mechanism and rate.

Figure 47 shows a collection of SEM images of unused and galvanostatically tested samples. The magnification is 500x. The sample after sulfuric acid test seems to be smoother than before the test. The samples after testing in copper or zinc containing solution have areas that seem to have lost part of the cracked mud surface features. This might be linked to the highest loss of surface charge as measured by cyclic voltammetry. The sample that has been tested in nickel containing solution seems also to have lost the cracked mud features and has some deep holes. It might be possible that even the active oxide from the outermost area is lost the active sites deeper in oxide structure can support oxygen evolution. The sample after testing in iron containing electrolyte seems to have quite identical morphology with the unused sample.

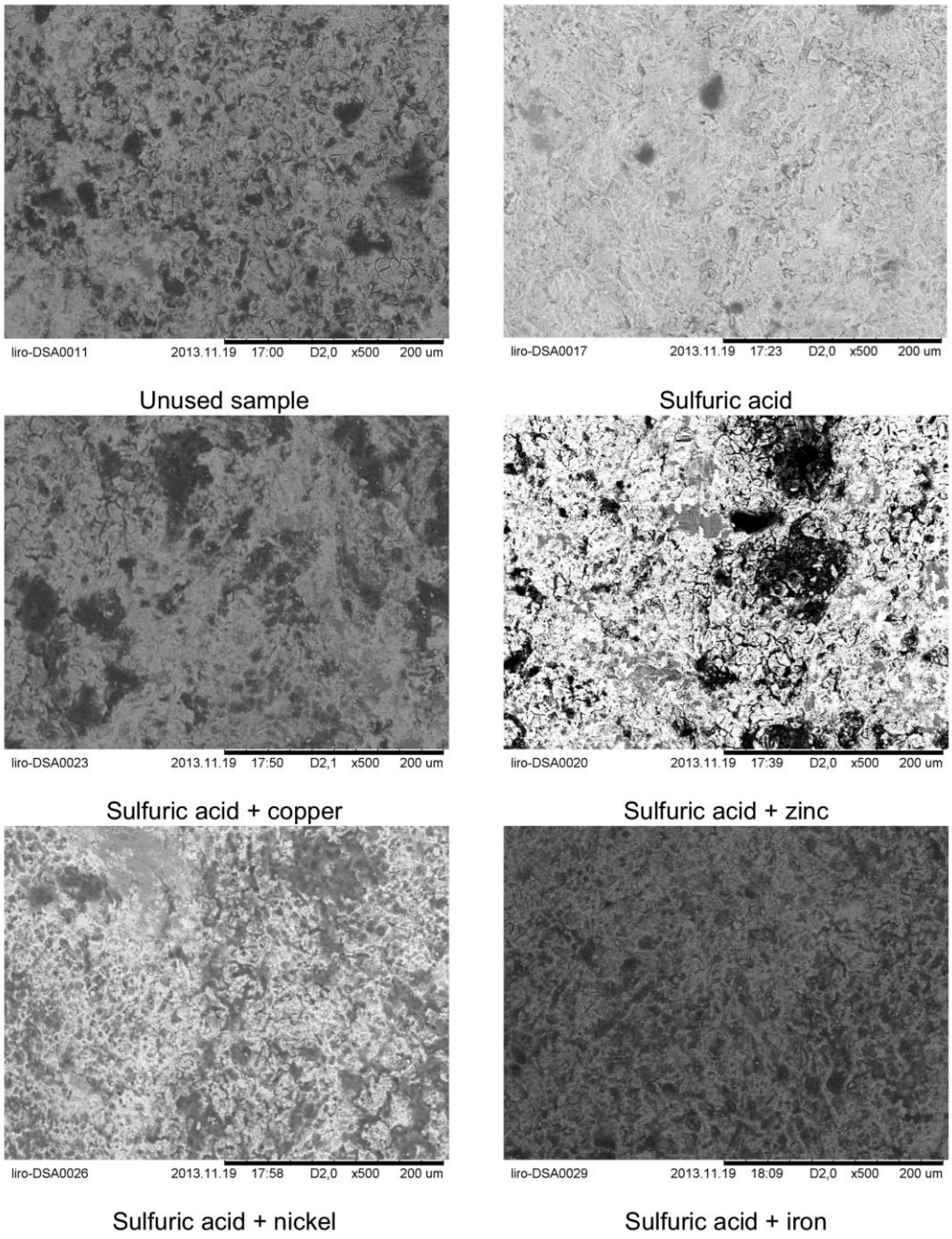

Figure 47. SEM images of tested samples.

8 DISCUSSION

The aim of this work was to estimate the effect of electrolyte properties on wear and corrosion of mixed metal oxide anodes. Based on literature the effects electrolyte composition, temperature and current density were evaluated by measuring and analyzing potentiodynamic polarization curves. The polarization curves were measured in 50, 100, 150 and 200 g/l sulfuric acid and in 100 g/l sulfuric acid with 20, 40 and 60 g/l copper, nickel, zinc or ferrous iron. In all electrolytes polarization curves were measured at temperatures 30, 40, 50 and 60 ºC. Anodes were thus tested in 64 different electrolytes. From the polarization curves it was possible to calculate Tafel slopes, activation energies and the effect of metal ion concentration on anode operating potential. The main tendencies found for sulfuric acid with or without copper, nickel or zinc are discussed first and the tendencies found with iron-containing electrolytes are discussed separately.

In most of the tested electrolytes an inflection point was detected around 100-300 A/m^2 and the Tafel slope was lower below this point and higher above this point. This change is due to change in the oxygen evolution mechanism [Fang 2010]. The Tafel slope values varied in the tested electrolytes. The average Tafel slope values at the low current density range both in sulfuric acid solutions and in 100 g/l sulfuric acid with copper, nickel or zinc were 54-56 mV. This value agrees with literature and indicates that at low current densities the metal ions do not affect oxygen evolution mechanism. At the high current density range the average Tafel slope value in sulfuric acid electrolytes without metal ions was 115 mV, in copper containing electrolytes 85 mV, in nickel containing electrolytes 97 mV and in zinc containing electrolytes 111 mV. The Tafel slope values were lower in metal-containing solutions than in sulfuric acid. However, no conclusions can be drawn from these results yet as the Tafel slope values in metal-containing electrolytes were scattered and no explanation on the effect of metal ions on oxygen evolution mechanism was found in the literature.

The effect of temperature was analyzed by calculating activation energies and constant potential below and above the inflection point. The selected potentials were 1.25 V and 1.35 V. The activation energies were in most cases between 20 kJ/mol and 30 kJ/mol indicating mixed control, where neither mass transfer nor charge transfer is clearly limiting the reaction rate. Mass transfer controlled reaction was found in concentrated sulfuric acid solution without metals at the high current density range. Generally, the metal ions were not seen to change the mechanism of anodic reaction.

The effect of sulfuric acid concentration was to increase the anode potential at constant current density or lower the current density at constant anode potential. The effect of acid concentration is probably linked to occupation of surface sites. Adsorption of sulfate molecules on anode surface will decrease the electrochemically active area. The effect of copper, nickel and zinc ions was the same as sulfate anions, but on much smaller scale. In all electrolytes a continuous increase of anode potential with increasing metal ion concentration was not detected.

The electrolytes containing ferrous iron showed different polarization curves than other ones tested in this thesis. At low potentials, before onset of oxygen evolution, the anodic reaction is oxidation of ferrous ion to ferric ion. The same effect was documented by [Ferrer 2013] when electrochemically producing ferric iron to be used as oxidant in sulfide leaching. Mass transfer controlled reaction was also in iron containing electrolytes at low potentials, but when oxygen evolution started the reaction was again under mixed control. Addition of iron to the electrolyte decreased clearly anode operating potential at potentials where both iron oxidation and oxygen evolution were proceeding.

The effect of metal and metal concentration on passivation were studied in galvanostatic tests. Tests were started using current density 500 A/m^2 that is close to the operating current densities of metal electrowinning processes. The current density was increased using 500 A/m^2 steps once a day. The final current densities were over 10 kA/m^2 in some tests. No passivation was noticed in any electrolyte. The anodes showed strongest wear and corrosion in copper and zinc containing electrolytes. In these tests the decrease of surface

charge and total charge, both linked to the number of active sites on the geometric area, was strongest and also the increase of charge transfer resistance that is inversely related to reaction rate was strongest. In nickel containing electrolytes same effects were seen but not as strongly. In iron containing electrolytes and metal free electrolytes the decrease of charge values was smallest and in these experiments the charge transfer resistance even decreased.

The anode samples withstood corrosion very well in the tested electrolytes. Even current densities that were ten times higher than used in electrowinning of base metals were not able to cause passivation in hundreds of hours. Therefore only few galvanostatic lifetime tests were done and their results are not conclusive. The activity measurements indicate that copper, zinc or nickel containing electrolytes do corrode anode faster than metal-free sulfuric acid electrolyte or iron-containing electrolyte that can support ferrous to ferric iron oxidation reaction. No explanation on the effect of metal ions on anode wear and corrosion rate was found as the metal ions were not found to alter the oxygen evolution mechanism.

In some galvanostatic tests the metal deposition on cathode was so strong that it resulted in short circuit between anode and cathode. These were detected when measured potential dropped to zero. The short circuits were corrected as soon as they were detected and tests were continued. Even multiple short circuits did not lead to loss of oxide film.

9 CONCLUSIONS

The mixed meal oxide anodes have been developed in the 1960's for chlor-alkali electrolysis and they have been proposed as replacement for lead anodes in metal electrowinning since 1970's. The metal oxide anodes have not been commercially successful in base metal production using sulfuric acid based electrolytes. The oxide anodes have been used successfully in chlorine based electrolytes like in cobalt production. The drawbacks of oxide anodes are considered to be higher cost, lower lifetime and sensitivity to short circuits.

The anode wear and corrosion mechanism has been developed in late 1990's and it includes initial loss of poorly attached particles, gradual increase in potential due to active metal dissolution and final passivation when potential is higher than that required for oxide film formation on base metal. The aim of this work was to find out if electrolyte conditions, especially metal ions, would change the active metal dissolution rate. One of the main factors affecting the dissolution rate is anode potential. The sulfuric acid concentration or metal ion concentration were not found to increase anode potential, but the addition of ferrous iron decreased anode potential. No changes in anode reaction mechanism were seen when analyzing the activation energies. The effect of metal ions on anode corrosion rate could not be ruled out, but the addition of metal ions did not cause a significantly higher potential that could initiate higher dissolution rate of the active iridium oxide.

Galvanostatic tests showed that anode activity decreased most clearly in sulfuric acid electrolytes containing copper or zinc. The same tendency was seen in nickel containing electrolytes but not as strongly. Anode activity decrease was detected as lower charge measured by cyclic voltammetry and higher charge transfer resistance measured by electrochemical impedance spectroscopy. These effects were not as clear in sulfuric acid without metals and in sulfuric acid with ferrous iron. These results indicate that the metal ions do have effect on anode corrosion rate but the mechanism was not clarified.

The test methods selected for anode activity determination worked well. Cyclic voltammetry at different sweep rates provided charge that is related to the active sites. More sweep rates could be used. Electrochemical impedance spectroscopy at constant potential provided clear charge transfer resistance results, but no changes in ohmic resistance or double layer capacitance happened. The selection of the test potential must be based on polarization curves so that the potential is clearly on oxygen evolution range. A major problem in anode testing is the selection of testing current density. The current densities used in electrowinning do not cause damages to the anodes. On the other hand, current densities that are tens of times higher do not lead to passivation in tens of hours. The solution could be use of extremely high current densities in the order of 10 kA/m^2, but they may no longer describe the same wear and corrosion phenomena that happen in metal electrowinning.

10 REFERENCES

Alves, V.A., da Silva, L.A., Boodts, J.F.C. (1998), Electrochemical impedance spectroscopic study of dimensionally stable anode corrosion. Journal of Applied Electrochemistry 28(1998), pp. 899-905.

Angelinetta, C., Trasatti, S., Atanasoska, Lj.D., Minevski, Z.S., Atanasoski, R.T. (1989), Effect of preparation on the surface and electrocatalytic properties of RuO_2+IrO_2 mixed oxide electrodes. Materials Chemistry and Physics 22(1989), pp. 231-247.

Ardizzone, S., Fregonara, G., Trasatti, S., "Inner" and "outer" active surface of RuO_2 electrodes. Electrochimica Acta 35(1990) 1, pp. 263-267.

Aromaa, J. (1994), On the corrosion of ruthenium oxide (RuO_2) based anodes in chloride solutions, Helsinki University of Technology, D.Sc. Thesis, TKK-V-A12, 1994, 79 p.

Aromaa, J., Pajunen, L., Forsén, O. (2002), Evaluation of the electrochemical activity of an insoluble anode. The International Jomar Thonstad symposium, Trondheim, Norway, 2002, p. 115-132.

Beck, F. (1989a), The wear mechanism of activated titanium anodes under current flow. Corrosion Science 29(1989) 2/3, pp. 379-387.

Beck, F. (1989b), Wear mechanisms of anodes. Electrochimica Acta 24(1989) 6, pp. 811-822.

Beer, H.B., Hinden, J.M. (1979), Päällystetty elektrodi, jossa on parannettu estokerros. Suom. Pat. FI 68090, 8.10.1979. 25 p.

Bock, C., Spinney, H., Macdougall, B. (2000). A study of the deactivation and service life of Ir oxide anodes supported on Al substrates. Journal of Applied Electrochemistry 30(2000), pp. 523-532.

Bondar, R.U., Kalinovskii, E.A. (1978), Electrochemical stability of titanium-ruthenium oxide anodes. Soviet Electrochemistry 14(1978) 5, pp. 633-636.

Cardarelli, F., Taxil, P., Savall, A., Comninellis, Ch., Manoli, G., Leclerc, O. (1998), Preparation of oxygen evolving electrodes with long service life under extreme conditions. Journal of Applied Electrochemistry 28(1998), pp. 245-250.

Chen, X., Chen, G. Yue, P.L. (2001), Stable Ti/IrO_x-Sb_2O_5-SnO_2 Anode for O_2 Evolution with Low Ir Content. Journal of Physical Chemistry B 105(2001), pp. 4623-4628.

Chen, X., Chen, G. (2005), Stable Ti/RuO_2–Sb_2O_5–SnO_2 electrodes for O_2 evolution. Electrochimica Acta 50(2005), pp. 4155–4159.

Comninellis, Ch., Vercesi, G.P. (1991), Characterization of DSA-type oxygen evolving electrodes: choice of a coating. Journal of Applied Electrochemistry 21(1991), pp. 335-345.

Da Silva, L.M., Fernandes, K.C., De Faria, L.A., Boodts, J.F.C. (2004), Electrochemical impedance spectroscopy study during accelerated life test of conductive oxides: Ti/(Ru + Ti + Ce)O_2-system. Electrochimica Acta 49(2004), pp. 4893–4906.

Endo, K., Katayama, Y., Miura, T., Kishi T. (2002), Composition dependence of the oxygen-evolution reaction rate on $Ir_xTi_{1-x}O_2$ mixed-oxide electrodes. Journal of Applied Electrochemistry 32(2002), pp. 173–178.

Fang, Y.H., Liu, Z.-P. (2010), Mechanism and Tafel Lines of Electro-Oxidation of Water to Oxygen on RuO_2(110). Journal of the American Chemical Society 132(2010), pp, 18214–18222.

Ferrer Muñoz, G. (2013), Electrochemical oxidation of refractory gold concentrate. Final Project, Aalto University, Department of Materials Science and Engineering. 60 p.

Galizzioli, D., Tantardini, F., Trasatti, S. (1974), Ruthenium dioxide: a new electrode material. I. Behaviour in acid solutions of inert electrolytes. Journal of Applied Electrochemistry 4(1974), pp. 57-67.

Galizzioli, D., Tantardini, F., Trasatti, S. (1975), Ruthenium dioxide: a new electrode material. II. Nonstoichiometry and energetic of electrode reactions in acid solutions. Journal of Applied Electrochemistry 5(1975), pp. 203-214.

Gorodetskii, V.V., Pecherskii, M.M., Yanke, V.B., Shub, D.M., Losev, V.V. (1979), Kinetics of dissolution of ruthenium – titanium oxide anodes in electrolysis of chloride solutions. Soviet Electrochemistry 15(1979) 4, pp. 471-474.

Gueneau de Mussy, J.-P., Macpherson, J.V., Delplancke, J.-L. (2003), Characterisation and behaviour of Ti/TiO_2/noble metal anodes. Electrochimica Acta 48(2003), pp. 1131-1141.

Hayfield, P.C.S. (1980), Elektrodi ja elektrolyyttinen kenno. Suom. Pat. FI 69123, 26.11.1980. 18 p.

Hine, F. (1985), Electrode Processes and Electrochemical Engineering. Plenum Press, New York 1985. 410 p.

Hine, F., Yasuda, M., Noda, T., Yoshida, T., Okuda, J. (1979), Electrochemical behavior of the oxide-coated metal anodes. Journal of the Electrochemical Society 126(1979) 9, pp. 1439-1445.

Hine, F., Yasuda, M., Yoshida, T. (1977), Studies on the oxide-coated metal anodes for chlor-alkali cells. Journal of the Electrochemical Society 124(1977) 4, pp. 500-505.

Hutchings, R., Müller, K., Kötz, R., Stucki, S. (1984), A structural investigation of stabilized oxygen evolution catalysts. Journal of material Science 19(1984), pp. 3987-3994.

Kelly, E.J., Vallet, C.E., White, C.W. (1990), Application of ion implication/RBS to the study of electrocatalysis. Comparison of chlorine evolution at Ir-implanted and Ru-implanted titanium electrodes. Journal of the Electrochemical Society 137(1990) 8, pp. 2482-2491.

Klementeva, V.S., Uzbekov, A.A. (1985), Dissolution of ruthenium and titanium at diferent ratios of their oxides in the coating of ruthenium-titanium oxide anodes. Societ Electrochemistry 21(1985) 6, pp. 736-738.

Kokoulina, D.V., Krasovitskaya, Yu.I., Ivanova, T.V. (1978), Oxygen evolution at ruthenium oxide anodes and its connection with anode destruction. Soviet Electrochemistry 14(1978) 3, pp. 398-401.

Kotowski, S., Parr, J. (1991), Titananoden für elektrochemische Prozesse. Metall 45(1991) 9, pp. 895-897.

Krysa, J., Kule, L., Mraz, R., Rousar, I. (1996), Effect of coating thickness and surface treatment of titanium on the properties of IrO_2-Ta_2O_5 anodes. Journal of Applied Electrochemistry 28(1996), pp. 99-105.

Kulandaisamy, S., Prabhakar Rethinaraj, J., Chockalingam, S.C., Visvanathan, S. Venkateswaran, K.V., Ramachandran, P., Nandakumar, V. (1997), Performance of catalytically activated anodes in the electrowinning of metals. Journal of Applied Electrochemistry 27(1997), pp. 579-583.

Kötz, R., Stucki, S. (1986), Stabilization of RuO_2 by IrO_2 for anodic oxygen evolution in acid media. Electrochimica Acta 31(1986) 10, pp. 1311-1316.

Lassali, T.A.F., Boodts, J.F.C., Bulhoes, L.O.S. (2000), Faradaic impedance investigation of the deactivation mechanism of Ir-based ceramic oxides containing TiO_2 and SnO_2. Journal of Applied Electrochemistry 30(2000), pp. 625-634.

Lodi, G., Sivieri, E., de Battisti, A., Trasatti, S. (1978), Ruthenium dioxide based film electrodes. III. Effect of chemical composition and surface morphology on oxygen evolution in acid solutions. Journal of Applied Electrochemistry 8(1978), pp. 135-143.

Loucka, T. (1977), The reason for the loss of activity of titanium anodes coated with layer of RuO_2 and TiO_2. Journal of Applied Electrochemistry 7(1977), pp. 211-214.

Matsumoto, Y., Sato, E. (1986), Electrocatalytic properties of transition metal oxides for oxygen evolution reaction. Materials Chemistry and Physics 14(1986), pp. 397-426.

Moats, M. (2008), Will Lead-Based Anodes Ever Be Replaced in Aqueous Electrowinning? JOM 60(2008) 10, pp. 46-49.

Nidola, A. (1981), Technological impact of metallic oxides as anodes. Electrodes of conductive metallic oxides, Part B, ed. S. Trasatti. Elsevier Scientific Publishing Company, Amsterdam 1981. pp. 627-659.

Onuchukwu, A.I., Trasatti, S. (1991), Effect of substitution of SnO_2 for TiO_2 on the surface and anode electrocatalytic properties of RuO_2+TiO_2 electrodes. Journal of Applied Electrochemistry 21(1991), pp. 858-862.

Pourbaix, M. (1966), Atlas of the Electrochemical Equilibria in Aqueous Solutions. Pergamon Press, London 1966. 644 p.

Savinell, R.F., Zeller III, R.L., Adams, J.A. (1990), Electrochemically Active Surface Area. Volammetric Charge Correlations for Ruthenium and Iridium Dioxide Electrodes. Journal of the Electrochemical Society 137(1990) 2, pp. 489-494.

Schrieber, C.F., Mussinelli, G.L. (1987), Characteristics and performance of the LIDA impressed current system in natural water and saline muds. Materials Performance 26(1987) 7, pp. 45-51.

Schultze, J.W. (1986), Grundlagen der Elektrokatalyse. In: Grundlagen von Elektrodenreaktionen, Dechema-Monographie 102(1986), ed. Schultze, J.W. Verlag Chemie, Weinheim 1986, pp. 273-296.

Shrivastava, P., Moats, M.S., (2008), Ruthenium Palladium Oxide-Coated Titanium Anodes for Low-Current-Density Oxygen Evolution. Journal of the Electrochemical Society 155(2008) 7, pp. E101-E107.

Trasatti, S., (1984) Electrocatalysis in the anodic evolution of oxygen and chlorine. Electrochimica Acta 29(1984) 11, pp. 1503-1512.

Trasatti, S. (1987), Oxide/aqueous solution interfaces, interplay of surface chemistry and electrocatalysis. Materials Chemistry and Physics 16(1987), pp. 157-174.

Xu, L.K., Scantlebury, J.D. (2003), Microstructure and Electrochemical Properties of IrO_2-Ta_2O_5-Coated Titanium Anodes. Journal of The Electrochemical Society, 150(2003) 6, pp. B254-B261.